Received: 24 September 2021 | Revised: 10 February 2022 | Accepted: 8 March 2022

DOI: 10.1111/jnc.15609

Journal of Neurochemistry JNC The Official Journal of the International Society for Neurochemistry WILEY

ORIGINAL ARTICLE

Copper bis(thiosemicarbazone) complexes modulate P-glycoprotein expression and function in human brain microvascular endothelial cells

Jae Pyun[1] | Lachlan E. McInnes[2] | Paul S. Donnelly[2] | Celeste Mawal[3] | Ashley I. Bush[3] | Jennifer L. Short[4] | Joseph A. Nicolazzo[1]

[1]Drug Delivery, Disposition and Dynamics, Monash Institute of Pharmaceutical Sciences, Monash University, Parkville, Victoria, Australia

[2]Bio21 Molecular Science and Biotechnology Institute, University of Melbourne, Parkville, Victoria, Australia

[3]Oxidation Biology Lab, Melbourne Dementia Research Centre, Florey Institute of Neuroscience and Mental Health, University of Melbourne, Parkville, Victoria, Australia

[4]Drug Discovery Biology, Monash Institute of Pharmaceutical Sciences, Monash University, Parkville, Victoria, Australia

Correspondence
Joseph A. Nicolazzo, Drug Delivery, Disposition and Dynamics, Monash Institute of Pharmaceutical Sciences, Monash University, 399 Royal Parade, Parkville, VIC., Australia.
Email: joseph.nicolazzo@monash.edu

Abstract

P-glycoprotein (P-gp) is an efflux transporter at the blood–brain barrier (BBB) that hinders brain access of substrate drugs and clears endogenous molecules such as amyloid beta (Aβ) from the brain. As biometals such as copper (Cu) modulate many neuronal signalling pathways linked to P-gp regulation, it was hypothesised that the bis(thiosemicarbazone) (BTSC) Cu-releasing complex, copper II glyoxal bis(4-methyl-3-thiosemicarbazone) (Cu^{II}[GTSM]), would enhance P-gp expression and function at the BBB, while copper II diacetyl bis(4-methyl-3-thiosemicarbazone) (Cu^{II}[ATSM]), which only releases Cu under hypoxic conditions, would not modulate P-gp expression. Following treatment with 25–250 nM Cu^{II}(BTSC)s for 8–48 h, expression of P-gp mRNA and protein in human brain endothelial (hCMEC/D3) cells was assessed by RT-qPCR and Western blot, respectively. P-gp function was assessed by measuring accumulation of the fluorescent P-gp substrate, rhodamine 123 and intracellular Cu levels were quantified by inductively coupled plasma mass spectrometry. Interestingly, Cu^{II}(ATSM) significantly enhanced P-gp expression and function 2-fold and 1.3-fold, respectively, whereas Cu^{II}(GTSM) reduced P-gp expression 0.5-fold and function by 200%. As both compounds increased intracellular Cu levels, the effect of different BTSC backbones, independent of Cu, on P-gp expression was assessed. However, only the Cu-ATSM complex enhanced P-gp expression and this was mediated partly through activation (1.4-fold) of the extracellular signal-regulated kinase 1 and 2, an outcome that was significantly attenuated in the presence of an inhibitor of the mitogen-activated protein kinase regulatory pathway. Our findings suggest that Cu^{II}(ATSM) and Cu^{II}(GTSM) have the potential to modulate the expression and function of P-gp at the BBB to impact brain drug delivery and clearance of Aβ.

Abbreviations: ABCB1, ATP-binding cassette sub-family B member 1; AD, Alzheimer's disease; ATP, adenosine triphosphate; Aβ, amyloid beta; BBB, blood–brain barrier; BTSC, Bis(thiosemicarbazone); Cu^{II}(ATSM), copper II diacetyl bis(4-methyl-3-thiosemicarbazone); Cu^{II}(GTSM), copper II glyoxal bis(4-methyl-3-thiosemicarbazone); DMSO, dimethyl sulphoxide; ERK1/2, extracellular signal-regulated kinases 1 and 2; MDR1, human gene for multidrug resistance protein 1 for P-glycoprotein / ABCB1; P-gp, P-glycoprotein; RRID, Research Resource Identifier (see scicrunch.org); RT-qPCR, reverse transcription quantitative real-time polymerase chain reaction.

KEYWORDS
Alzheimer's disease, bis(thiosemicarbazone), blood–brain barrier, copper, efflux transporters, P-glycoprotein

1 | INTRODUCTION

The blood–brain barrier (BBB) is a highly selective gateway regulating the influx of molecules from the systemic circulation into the brain and the efflux of molecules in the reverse direction (Hawkins & Davis, 2005). The BBB is anatomically defined by highly specialised brain endothelial cells that line the complex network of cerebral microvasculature perfusing the brain (Abbott et al., 2010). These cells express numerous efflux transporter proteins on the luminal (blood-facing) surface, forming a biochemical barrier protecting the brain from potential xenobiotic infiltration (Nicolazzo et al., 2006). One of the most abundant and renowned transporters known for its broad-substrate specificity leading to multidrug resistance is P-glycoprotein (P-gp) (Schinkel, 1999). P-gp is an ATP-binding cassette (ABC) transporter encoded by the human multidrug 1 resistance (MDR1) gene (Juliano & Ling, 1976; Ueda et al., 1987). P-gp has been termed the 'gatekeeper' to the brain because of its role in preventing a multitude of endogenous molecules as well as drugs from entering into the brain (Schinkel, 1999). Numerous studies have compared the brain uptake of structurally diverse compounds in P-gp deficient versus wild-type mice. There have been observations of up to 100-fold increases in the brain accumulation of P-gp substrates (e.g. ivermectin, vinblastine and loperamide) in P-gp deficient mice relative to wild-type mice, outcomes associated with increased neurotoxicity of these drugs (Kannan et al., 2010; Kusuhara et al., 1997; Schinkel et al., 1994; Schinkel et al., 1995; Schinkel et al., 1996). While this effect has been observed for many other drugs, countless approaches to inhibit P-gp-mediated BBB efflux of drugs as a mechanism to enhance central nervous system (CNS) access of therapeutics has failed to improve clinical outcomes (Atadja et al., 1998; Callaghan et al., 2014; Palmeira et al., 2012). Therefore, novel approaches to regulate P-gp expression and function are warranted to overcome the negative impact of this efflux transporter on the delivery of drugs into the CNS.

In addition to the role that P-gp plays in limiting CNS drug delivery, there is growing evidence that dysregulation of P-gp expression and function at the BBB contributes to the pathophysiology of neurodegenerative diseases including, but not limited to, Alzheimer's disease (AD) (Karamanos et al., 2014; Qosa et al., 2016; van Assema et al., 2011; Vautier & Fernandez, 2009). P-gp has been shown to mediate the clearance of amyloid beta (Aβ), the toxic peptide that accumulates in the brain of individuals with AD (Kuhnke et al., 2007; Lam et al., 2001). Using a transgenic P-gp deficient mouse model, one study demonstrated increased accumulation of exogenously administered Aβ in the hippocampal region, and administration of a P-gp inhibitor elevated endogenous brain Aβ levels in an AD mouse model (Cirrito et al., 2005). Furthermore, recent functional studies have used isolated brain capillaries from mice as well as cellular models to demonstrate P-gp-mediated transport of fluorescent Aβ, which was significantly reduced in the presence of P-gp inhibitors (Chai et al., 2021; Hartz et al., 2010). Compelling evidence suggests that a decrease in P-gp expression at the BBB is part of the pathophysiology of AD, which ultimately impairs the capacity for normal Aβ clearance, a pathological hallmark of AD (Deo et al., 2014; Vogelgesang et al., 2002). For example P-gp expression has been shown to be inversely correlated with brain Aβ accumulation and deposition (Chiu et al., 2015; Wijesuriya et al., 2010). In post-mortem brain samples, regions where there was an abundance of P-gp in brain microvessels were associated with diminished Aβ plaque burden when compared with the same regions of non-AD individuals (Deo et al., 2014; Jeynes & Provias, 2011). The efflux function of P-gp has also been shown to be diminished in AD using positron emission tomography (PET) imaging with the P-gp substrate [^{11}C]verapamil, where increased brain accumulation of this substrate was observed in individuals with AD relative to those without AD (van Assema et al., 2011). Furthermore, it has been shown that targeting intracellular signals known to up-regulate and restore P-gp in brain capillaries lead to a reduction in Aβ accumulation in a mouse model of AD (Hartz et al., 2010). Taken together, these studies suggest that approaches aimed at increasing P-gp expression and function could increase the clearance of Aβ and therefore attenuate amyloid burden in individuals with AD.

Our laboratory has recently shown that an increase in human brain microvascular intracellular copper (Cu) was associated with an increase in the expression and function of P-gp (McInerney et al., 2018). This association was observed in immortalised human brain endothelial (hCMEC/D3) cells that were treated with a combination of Cu, zinc (Zn) and clioquinol (CQ), a metal chaperone which has been shown to bind to divalent metal cations and increase their uptake into neuronal cells (Crouch et al., 2011). However, in our previous studies, it could not be concluded that the positive effects of this combination of CQ, Cu and Zn on P-gp expression and function were purely Cu-mediated given that CQ can bind to other divalent metal ions, and has limited control over release and retention of cellular levels (Cherny et al., 2001; Donnelly et al., 2008). Therefore, as a way to more clearly ascertain the role of Cu on P-gp expression and function in hCMEC/D3 cells, the current study employed copper II bis(thiosemicarbazone) complexes (Cu^{II}(BTSCs)), a group of compounds that are designed to deliver exogenously bound Cu directly into cells (Donnelly et al., 2008). The copper II glyoxal bis(4-methyl-3-thiosemicarbazone) (Cu^{II}(GTSM)) (Figure 1a) variant of the compound is known to readily release Cu and has been shown in various studies to activate pathways for which Cu is a key cofactor (Acevedo et al., 2018; Bica et al., 2014; Crouch et al., 2009;

Donnelly et al., 2008). The mitogen-activated protein kinase (MAPK) pathway and the downstream activation of extracellular signal-regulated kinases (ERK1/2) has been shown to be affected by Cu^{II}(BTSC)s (Acevedo et al., 2018; Crouch et al., 2009; Srivastava et al., 2016) and these pathways have been demonstrated to regulate P-gp expression (Nwaozuzu et al., 2003; Shao et al., 2016; Zhou et al., 2019). Furthermore, others have shown that Cu^{II}(GTSM) enhances neuronal bioavailability of Cu, leading to inhibition of glycogen synthase kinase 3 beta (GSK3β) (Hickey et al., 2011), a pathway which has been shown to regulate P-gp expression at the BBB (Harati et al., 2012; Lim et al., 2008; Shen et al., 2013). It is, therefore, possible that Cu released from Cu^{II}(GTSM) could impact these signalling pathways at the BBB, resulting in increased BBB expression of P-gp.

The aim of this study, therefore, was to assess the impact of increasing bioavailable Cu via Cu^{II}(GTSM) on the expression and function of P-gp in hCMEC/D3 cells as a model of the BBB. Copper II diacetyl bis(4-methyl-3-thiosemicarbazone) (Cu^{II}(ATSM)), a compound similar in structure to Cu^{II}(GTSM) (Figure 1b) was used as an intended negative control as it has previously been shown to not readily release Cu under normal conditions and only releases the exogenously bound Cu under hypoxic conditions (Dearling et al., 2002; Donnelly et al., 2008; Xiao et al., 2008). These studies, therefore, have the potential to modulate a key efflux transporter at the most important biological barrier protecting the brain not only to modulate the delivery of therapeutics into the CNS but also to enhance the brain clearance of Aβ.

2 | MATERIALS AND METHODS

2.1 | Materials

Dimethyl sulphoxide (DMSO) (Cat# 41640, 2018), beta-mercaptoethanol (β-ME) (Cat# 63689, 2017) glycine (Cat# G8898, 2019), glycerol (Cat# G5516, 2019), sodium dodecyl sulphate (SDS) (Cat# L3771, 2018), thiazolyl blue tetrazolium bromide (MTT) (Cat# M5655, 2019), ammonium persulphate (APS) (Cat# A3678, 2017), tetramethylethylenediamine (TEMED) (Cat# T9281, 2016), tris base (TRIZMA® base) (Cat# T1503, 2019), sodium chloride (Cat# S3014, 2019), Triton® X-100 (Cat# T8787, 2018), Tween® 20 (Cat# P2287, 2019), rhodamine 123 (R123) (Cat# R8004, 2018), Dulbecco's phosphate buffer saline (D-PBS) (Cat# D8537, 2018), cOmplete™ mini protease inhibitor (Cat# 04693124001, 2018), phosSTOP™ phosphatase inhibitor cocktail tablets (Cat# 4906845001, 2020) and trypan blue (Cat# T8154, 2018) were purchased from Sigma-Aldrich (St Louis, MO). The fluorometric LDH assay kit (Cat# AB197000, 2019) was purchased from Abcam (Cambridge, UK). Hank's Balanced Salt Solution (HBSS) (Cat# 14175095, 2020), Pierce™ bicinchoninic acid (BCA) protein assay kit (Cat# 23225, 2019) and Pierce™ IP lysis buffer (Cat# 87788, 2019) composed of 25 mM Tris–HCl pH 7.4, 150 mM NaCl, 1 mM EDTA, 1% *(w/v)* NP-40 and 5% *(v/v)* glycerol were purchased from Thermo Fisher Scientific (Rockford, IL). HyClone bovine serum albumin (BSA) (Cat# SH30574.02, 2020) was purchased from GE Healthcare Life Sciences (Little Chalfont, UK). 0.45 μm nitrocellulose membranes (Cat# 1620115, 2018) and low fluorescence PVDF 0.45 μm membrane (Cat# 1620264, 2020), 40% *(v/v)* acrylamide/bis solution (37:1) (Cat# 161–0148, 2017), Precision Plus Protein™ Dual Xtra Standards (Cat# 1610377, 2018), Mini-Protein® TGX™ Precast gels (4–15% acrylamide) (Cat# 4561084, 2019) and extra thick blot paper (Cat# 1703960, 2019) were purchased from Bio-Rad (Hercules, CA). Primary C219 monoclonal antibody for P-gp (Cat# 903701, RRID: AB_2565033, 2018) was purchased from BioLegend® and the primary mouse antibody for β-actin (Cat# ab3280, RRID: AB_303668, 2018) was purchased from Abcam (Cambridge, UK). Primary antibody for total p44/42 MAPK (ERK1/2) (Cat# 9102, RRID: AB_330744, 2020) and phospho-p44/42 MAPK (pERK1/2) (Cat# 9101, RRID: AB_331646, 2020) were purchased from Cell Signalling Technology (Danvers, MA). The MEK1/2 inhibitor U-0126 (Cat# 70970, 2020) was purchased from Cayman Chemical (Ann Arbor, MI). Odyssey blocking buffer in PBS (Cat# LCR-927-40000, 2018 discontinued), Intercept® blocking buffer in PBS (Cat# LCR-927-70003, 2020), IRDye® 800CW goat anti-mouse (Cat# 926–32210, RRID: AB_621842, 2018) and IRDye® 680LT donkey anti-rabbit (Cat# 926–68023, RRID: AB_10706167, 2018) secondary antibodies, Intercept® blocking buffer and antibody diluent in TBS (Cat# LCR-927-60001, 2020) were purchased from LI-COR. RNeasy® Plus mini kit (Cat# 74136, 2019) was purchased from Qiagen. TaqMan® primer/probes for human MDR1 (sequence ID Hs01067802_m1, FAM), β-actin (sequence ID Hs_01060665_g1, FAM) and glyceraldehyde 3-phosphate dehydrogenase (GAPDH) (sequence ID = Hs0227258991_g1, FAM) (Cat# 4331182, 2020) were purchased from Applied Biosystems, Thermo Fisher Scientific. The immortalised human cerebral microvascular endothelial cell line (hCMEC/D3, RRID: CVCL_U985) (Weksler et al., 2005) was kindly provided by Dr. Pierre-Olivier Couraud (Inserm, Paris, France). This cell line was not authenticated by the authors and is not listed as a commonly misidentified cell line by the International Cell Line Authentication Committee (ICLAC). Endothelial basal medium-2 (EBM2) media (Cat# 190860, 2018) was used for all hCMEC/D3 cell culture experiments and this growth media were supplemented with a growth factor kit (Cat# CC-4176, 2018) prior to cell seeding, proliferation and experiments: 0.01% *(v/v)* ascorbic acid, 0.01% *(v/v)* gentamicin/amphotericin, 0.01% *(v/v)* hydrocortisone, 0.025% *(v/v)* epidermal growth factor, 0.025% *(v/v)* insulin-like growth factor, 0.025% *(v/v)* vascular endothelial growth factor and 0.1% *(v/v)* b-splice variant fibroblast growth factor purchased from Lonza (Walkersville, MD), 10 mM HEPES (Cat# H4034, 2018), 1% *(v/v)* penicillin/streptomycin (Cat# P4458-100ML, 2018) and 2.5% *(v/v)* fetal bovine serum (FBS) (Cat# 12003C, 2018) were purchased from Sigma-Aldrich (St Louis, MO). 0.25% trypsin–EDTA *(w/v)* (Cat# 25200072, 2018) was purchased from Thermo Fisher Scientific (Rockford, IL). Rat-tail collagen Type I (Cat# FAL354236, 2018) and all plastic cell culture equipment including T75 flasks and 6-96-well plates were purchased from Corning (Corning, NY). The P-gp inhibitor PSC833 was a gift from Novartis (Basel, Switzerland).

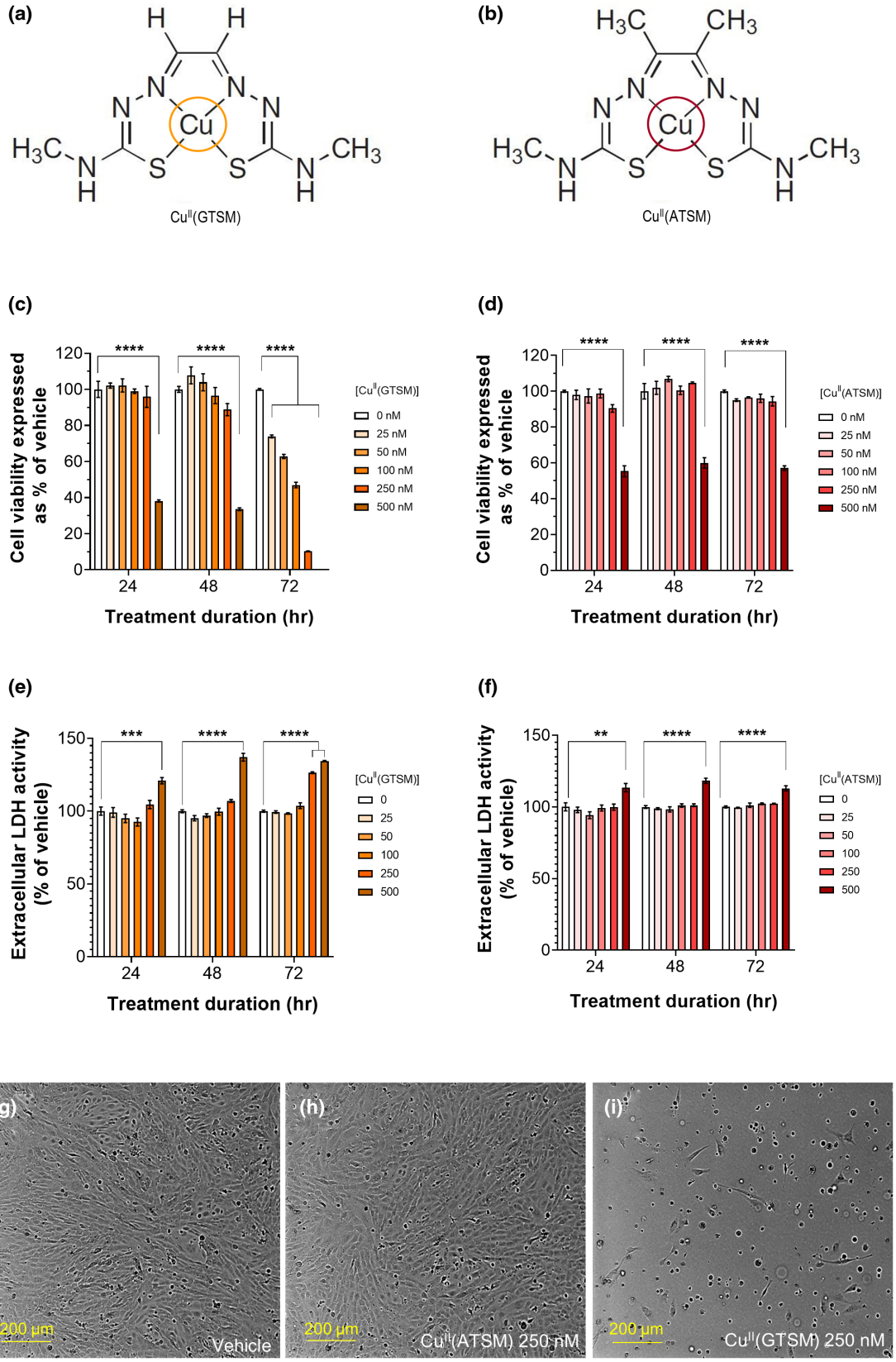

2.1.1 | Bis(thiosemicarbazone) complexes

The BTSC compounds Cu^{II}(GTSM) (Beraldo et al., 1997; Blower et al., 2003; Dearling et al., 2002), Cu^{II}(ATSM), H_2(ATSM), (Blower et al., 2003; Dearling et al., 2002; Gingras et al., 1962; West et al., 1997) and Ni^{II}(ATSM) (Jones & McCleverty, 1970; Southon et al., 2020; West et al., 1997) were synthesised as described previously. hCMEC/D3 cells were treated with Cu^{II}(BTSC) complexes at

FIGURE 1 Structure of copper bis(thiosemicarbazone) complexes (a) copper II glyoxal-bis(N[4]-methylthiosemicarbazonato) (Cu^{II}(GTSM)) and (b) copper II diacetyl-bis(N[4]-methylthiosemicarbazonato) (Cu^{II}(ATSM)). (c, d) MTT cell viability assays and (e, f) LDH cytotoxicity assays following 24–72 h treatment with 25–500 nM Cu^{II}(GTSM) (c, e) or Cu^{II}(ATSM) (d, f). A vehicle control with 0.1% *(v/v)* DMSO was used. Brightfield microscopic representations of hCMEC/D3 cells following a 72 h treatment with (g) vehicle, (h) 250 nM of Cu^{II}(ATSM) or (i) Cu^{II}(GTSM). Data are presented as mean ± SEM ($n = 4–5$, independent cell culture preparations for each timepoint) expressed as a % of vehicle (0.1% *(v/v)* DMSO) for each timepoint. $^{**}p < 0.01$, $^{***}p < 0.001$, $^{****}p < 0.0001$ when compared with vehicle-treated cells assessed by a one-way ANOVA followed by a post hoc Dunnett's test. Note: Each timepoint are individual experiments and were statistically analysed as separate experiments and are represented together to capture the change with treatment times. Individual data points are not presented because of the tightness of the data

a range of concentrations to assess P-gp expression and function. All stock BTSC compounds were dissolved in sterile DMSO and diluted in EBM2 media with 0.1% *(v/v)* DMSO in the final working solutions.

2.2 | Methods

2.2.1 | Culturing of cells and treatments

hCMEC/D3 cells were kept cryogenically frozen in vapour phase in a cryo-storage solution consisting of 5% *(v/v)* DMSO in heat-inactivated FBS prior to resuscitation. Before seeding cells, T75 flasks were pre-coated with 4 ml of a 0.1 mg/ml solution of collagen type I and incubated for 1 h, before being washed with 10 ml of PBS. Vials containing approximately 1 million cells/ml of the cryo-storage solution were dispensed into T75 flasks containing 14 ml of EBM2 media supplemented with the aforementioned growth factors. Once seeding was complete (2 h), the media were aspirated off and replaced with fresh pre-warmed media to remove trace DMSO from the cryo-storage solution. Cells were incubated at 37°C and 5% CO_2, and the media were changed every 2 days until the flasks reached approximately 90–100% confluence (approximately 4 days). Cells grown to confluence were rinsed twice with 10 ml of PBS after spent media removal, before being treated with 4 ml of trypsin/EDTA solution, and incubated at 37°C for 4 min. This was followed by the addition of 11 mL of solution containing 2.5% *(v/v)* FBS in PBS to halt the trypsinisation process. Cells were removed and transferred to a 50 mL Falcon tube and an 80 µl aliquot of the cell suspension was combined with 20 µl of trypan blue staining solution and counted on a haemocytometer. The cell suspension was transferred to an *Eppendorf 5810R* centrifuge chamber and centrifuged at 650 rcf for 5 min. The supernatant was removed and pelleted cells were homogenised and diluted in an appropriate volume of pre-warmed EBM2 media, such that the volume to be transferred to any plate used throughout experiments would correspond to a cell seeding density of 20000 cells/cm^2. Experiments were conducted in 6-well plates for mRNA and protein expression, 24-well plates for determination of intracellular metal concentrations, 48-well plates for P-gp functional studies and 96-well plates for cell viability assays. All experiments performed using the hCMEC/D3 cell line occurred between passages 27–35 to minimise the potential of phenotypic changes as advised by Weksler et al. (Weksler et al., 2005). ARRIVE guidelines were not followed because no animals were used in the current study.

2.2.2 | Assessment of cell viability and toxicity in response to Cu^{II}(GTSM) and Cu^{II}(ATSM)

hCMEC/D3 cells seeded into 96-well plates at 20000 cells/cm^2 were treated for different durations and halted at approximately 100% confluence (72 h). The treatment times were 8, 24, 48 and 72 h with Cu^{II}(GTSM) or Cu^{II}(ATSM) at concentrations ranging from 25 to 500 nM. After the treatment period, cells were washed with warm PBS and then incubated with 0.45 mg/ml MTT reagent solution in blank EBM2 media for 4 h to allow the mitochondrial reductase enzymes of viable cells to reduce MTT to purple formazan. Following incubation, the MTT reagent was carefully removed and replaced with 150 µl of DMSO and shaken on an agitator for a further 30 min. 10% (*v/v*) DMSO treatment was used as a positive control to induce cell death and background absorbance was obtained by adding MTT reagent to wells containing no cells. Absorbance was read at 540 nm using the Enspire absorbance spectrophotometer (PerkinElmer, Waltham, MA). Background absorbance was subtracted from all other wells before analysis and the absorbance of treatment groups was averaged and normalised against the average of vehicle (0.1% *(v/v)* DMSO) controls to be comparatively expressed as a percentage of cell viability.

To account for the variance in cell density with treatment times and the observable detachment of cells following Cu^{II}(BTSC) treatments, lactate dehydrogenase (LDH) activity was also measured to assess cellular damage and cytotoxicity. The LDH assay followed standard operating procedures according to the manufacturer's protocols. In brief, hCMEC/D3 cells were treated identically to the MTT assays for 24, 48 and 72 h treatments with Cu^{II}(BTSC) complexes. A 10 µl aliquot of cell media was taken and diluted 1:5 with LDH assay buffer to a total sample volume of 50 µl and plated on to a clear flat-bottom 96-well plate along with equal volumes of known concentration of NADH standards. To each well, a 50 µl aliquot of reaction mix (91% *(v/v)* LDH assay buffer, 5% *(v/v)* PicoProbe and 4% *(v/v)* LDH substrate mix) was added and incubated at 37°C for 10 min and then measured on the Enspire fluorescence spectrophotometer at excitation and emission wavelengths of 535 and 587 nm, respectively. Samples were blank corrected, and concentrations were determined from a validated standard curve of NADH standard solutions of known concentrations. The extracellular LDH activity for each well was expressed as a percentage of the LDH activity from the vehicle control (0.1% *(v/v)* DMSO).

2.2.3 | Measurement of MDR1 mRNA using quantitative real-time PCR (RT-qPCR)

To identify changes in MDR1 gene expression in response to Cu^{II}(BTSC) treatments, quantitative reverse-transcriptase real-time polymerase chain reaction (RT-qPCR) was performed on RNA isolated from treated hCMEC/D3 cells. Following treatments, cells were washed twice with ice-cold PBS and total RNA was isolated using the RNeasy Plus Mini Kit (Qiagen, Hilden, Germany), as per the manufacturer's protocol. RNA concentration (absorbance at 260 nm) and purity were determined using the NanoDrop® 1000 spectrophotometer (Thermo Fisher Scientific), with the purity determined via assessment of 260/280 and 260/230 ratios. Each RNA sample was diluted to 20 ng/μl with RNase-free water and 5 μl aliquots were dispensed into a 96-well plate, to which the following was added: 20 μl of a mastermix solution containing 12.5 μl of 2x probes RT-PCR reaction mix, 0.5 μl of iScript™ reverse transcriptase, 6.305 μl of nuclease-free water and 0.695 μl of either MDR1, GAPDH or β-actin TaqMan probes. Measurement of gene amplification was carried out in the Bio-Rad CFX96 C1000™ Thermal Cycler (Bio-Rad). Thermocycling was initiated at 50°C for 10 min, 95°C for 5 min and followed by a total of 50 cycles at 95°C for 15 s and 60°C for 30 s. The fluorescence detected from the MDR1 gene at the threshold cycles (C_t) was normalised to the geometric mean of the C_t values for the two reference genes GAPDH and β-actin to determine the relative fold-change ($2^{-\Delta\Delta Ct}$) of MDR1 mRNA in treated cells compared to vehicle controls (0.1% *(v/v)* DMSO) (Livak & Schmittgen, 2001).

2.2.4 | Quantification of P-gp protein using Western blot analysis

Following treatment with Cu^{II}(BTSC) complexes or vehicle (0.1% *(v/v)* DMSO) (8, 24 or 48 h), hCMEC/D3 cells were lysed with 200 μl of Pierce™ IP lysis buffer supplemented with the cOmplete™ mini protease inhibitor cocktail for 30 min at 4°C. Cell lysates were obtained with a cell scraper and transferred to a pre-cooled Eppendorf tube and centrifuged at 14 000 rcf for 10 min. The supernatant was collected and the total protein content in the sample was determined according to the Pierce™ BCA protein assay kit procedures with known BSA standards used to generate a standard curve previously validated for accuracy and precision. The appropriate volume for each sample corresponding to 15 μg of protein was vortexed with loading (Laemmli) buffer (20% *(w/w)* glycerol, 0.125 M Tris–HCl buffer, 10% *(v/v)* SDS, 0.5% *(v/v)* bromophenol blue and 25% *(v/v)* β-mercaptoethanol in milliQ (MQ) water), in a ratio of 5:1 and incubated at 37°C for 30 min. The samples were centrifuged at 14000 rcf for 2 min and then pipetted from the microfuge tubes into lane wells of Mini-Protein® TGX™ Precast gels (4–15% acrylamide) in random order to avoid gel effects and then assembled into the Bio-Rad mini protean tetra cell (Hercules, CA), with 3 μl of the Dual Xtra Precision Plus Protein Prestained Standards ladder included. The gel and buffer dam apparatus were submerged in ice-cold running buffer (25 mM Tris base, 190 mM glycine and 0.1% *(w/v)* SDS in MQ water) and set to a pH of 8.2. Gel electrophoresis was run at 150 V for 90 min. The gel was removed from the electrophoresis apparatus and incubated with the 0.45 μm pore-sized nitrocellulose membrane and extra thick blotting paper in transfer buffer (25 mM Tris buffer, 190 mM glycine and 10% *(v/v)* methanol) for 20 min. Protein transfer was executed using the Bio-Rad Trans-Blot Turbo transfer system (Hercules, CA) set to 25 V and 1.0 A for 40 min. After completion of the transfer, the nitrocellulose membrane was rinsed briefly with tris-buffered saline (TBS) containing 0.1% *(v/v)* Tween 20 (TBST) and then incubated in LI-COR Odyssey blocking buffer at room temperature (20–22°C) for 1 h. The membrane was then rinsed briefly in TBST and co-incubated with primary antibodies specific for β-actin and P-gp diluted in 10 ml of TBST (1:500000 and 1:500 respectively) under gentle agitation overnight at 4°C. Membranes were washed thoroughly in TBST 5 times for 5 min on an agitator before 15 ml of the secondary IRDye® 800CW goat anti-mouse and IRDye® 680LT donkey anti-rabbit antibody in TBST were applied (dilution of 1:7500 and 1:15000, respectively) for 2 h at room temperature (20–22°C) in a light proof container under gentle agitation. The wash step was repeated followed by detection of the protein bands using the LI-COR Odyssey Infrared Imaging system (Lincoln, NE). Densitometric analysis of the P-gp and β-actin bands of interest was conducted using ImageJ software (National Institutes of Health, Bethesda, MD). P-gp band intensities were normalised to the housekeeping β-actin and expressed as relative fold-change to lanes with vehicle controls.

2.2.5 | Activation of ERK1/2 assessed by Western blot analysis

Following treatment with Cu^{II}(ATSM) or Cu^{II}(GTSM) for 24 h, hCMEC/D3 cells were lysed using the same procedure described above with the addition of a phosphatase inhibitor (phosSTOP™) in the lysis buffer. The membrane was replaced with a 0.45 μm pore size low-fluorescence PVDF membrane that was activated with absolute methanol prior to the transfer step. The transfer was run at 25 V and 1.0 A for 25 min. The membrane was incubated in the Intercept blocking buffer in TBS for 1.5 h at room temperature (20–22°C) in a light proof container under gentle agitation. Following blocking, the membrane was probed for pERK at a 1:1000 dilution in LI-COR antibody diluent (0.2% *(w/v)* Tween 20) under gentle agitation overnight at 4°C. The next day, the membrane was washed as previously described and incubated with secondary donkey anti-rabbit IRDye 690LT in antibody diluent (1:10000) supplemented with 0.01% *(v/v)* SDS for 1.5 h at room temperature (20–22°C) and subsequently washed in TBST and imaged on the GE Amersham™ Typhoon™ scanner. The membrane was then retained to be stripped (using 0.2 M NaOH) of pERK antibodies and re-probed for total ERK following the same procedures described and then finally for the housekeeping protein β-actin. The corresponding bands were analysed for densitometric quantification using ImageJ software and expressed as a ratio of pERK:ERK to show activation of ERK1/2.

2.2.6 | Assessing P-gp function through R123 accumulation

The impact of Cu^{II}(BTSC) complexes on P-gp function in hCMEC/D3 cells was determined by measuring the accumulation of the widely used fluorescent P-gp substrate R123. Once cells reached the appropriate confluence for timepoint studies (70–80% for 24 h treatments, 50–60% for 48 h treatments), the media were removed and the cells were treated with 250 µl/well of Cu^{II}(ATSM) or Cu^{II}(GTSM) at a concentration of 25–250 nM or with vehicle (0.1% *(v/v)* DMSO in media). Following treatment, cells were rinsed twice with 250 µl/well of pre-warmed PBS and incubated with transport buffer (10 mM HEPES in HBSS pH 7.4) containing vehicle (0.1% *(v/v)* DMSO) or 5 µM PSC833 (valspodar) (a known P-gp inhibitor) (Atadja et al., 1998) at 37°C and 5% CO_2 under constant agitation for 15 min. Cells were then rinsed with 250 µl/well of pre-warmed transport buffer and replaced with 5 µM R123 in transport buffer ±5 µM PSC833. The plate was then incubated at 37°C, 5% CO_2 under constant gentle agitation for 60 min. Following this R123 incubation, cells were rinsed 3 times with 250 µl/well of ice-cold transport buffer and then lysed with 100 µl of ice-cold lysis buffer (1% *(v/v)* Triton X-100 in MQ water) on a plate shaker for 20 min at 4°C. 50 µl of known R123 standards (prepared in 1% *(v/v)* Triton® X-100 in MQ water) as well as 50 µl of the lysates from each well were then transferred into a 96-well plate and R123 fluorescence was detected using an Enspire fluorescence spectrophotometer at excitation and emission wavelengths of 511 and 534 nm, respectively. Raw fluorescence values were blank corrected with wells containing 1% *(v/v)* Triton X-100 in MQ water to account for background detection. The fluorescence readings of cellular lysates were then compared to known standard solutions of R123 plated onto the same 96-well plate. The mass of fluorescent R123 (nmol) was then normalised to total cellular protein determined using the Pierce™ BCA protein assay (mg) and the accumulation (nmol/mg) was compared between vehicle and treated cells.

As it could be argued that the effect of Cu^{II}(GTSM) could have been a result of direct inhibition of P-gp-mediated efflux (as described in Results), R123 uptake was measured in the presence and absence of Cu^{II}(GTSM). R123 (5 µM) was co-incubated with Cu^{II}(GTSM) (100 nM) with or without PSC833 (5 µM) in untreated hCMEC/D3 cells. Accumulation was measured following 2, 15, 30, 45 and 60 mins of incubation followed by protein and fluorescence readings performed as described for the aforementioned functional studies.

2.2.7 | Detection of intracellular copper by inductively coupled plasma mass spectrometry (ICP-MS)

hCMEC/D3 cells were seeded in 24-well plates using the protocol for cell seeding described above. For every treatment replicate, it was necessary to have one blank replicate that contained no cells. Blanks were treated identically throughout the process (lysed the same way, as though they had cells in them), and were used to blank correct for background metal detection. Following treatment, cells were washed twice with 500 µl of ice-cold PBS, then lysed with 250 µl of ice-cold 1% *(v/v)* Triton X-100 in MQ water and put on a shaker at 4°C for 15 min. Following lysis, the lysate was homogenised and 240 µl was transferred to pre-cooled Eppendorf tubes. For blank-treated wells, only 210 µl of the lysis solution was transferred to the labelled Eppendorf tubes as protein analysis was not necessary. Cell lysate samples were quantified for protein using the Pierce™ BCA assay using 30 µl aliquots so that the remaining total sample volumes would be consistent at 210 µl. Samples were then freeze-dried and 50 µl of concentrated nitric acid 65% *(v/v)* was added for digestion overnight at room temperature (20–22°C). The next day, samples were heated at 90°C for 20 min to complete the digestion, leaving a volume after digestion of approximately 40 µl. To each sample, 960 µl of 1% *(v/v)* of nitric acid diluent was added to a final volume of 1 ml. The samples were injected onto an Agilent 7700 series ICP-MS instrument (Agilent Technologies) under routine multi-element operating conditions using a Helium Reaction Gas Cell. The instrument was calibrated using 0, 5, 10, 50, 100 and 500 ppb of certified multi-element ICP-MS standard calibration solutions (ICP-MS-CAL2-1, ICP-MS-CAL-3 and ICP-MS-CAL-4, Accustandard, New Haven, CT) for a range of elements. A certified standard solution containing 200 ppb of Yttrium (Y89) was used as an internal control (ICP-MS-IS-MIX1-1, Accustandard). Raw ppb data of the elements were converted to µmol/L with dilution factors applied. Final concentrations of metals (µmol/L) were then blank corrected with treatment blanks and normalised to total protein obtained from the BCA assay. The final unit expressed as a percentage of the control was nmol of Cu/mg protein.

2.2.8 | Assessing the effect of ATSM backbone controls on copper uptake and P-gp expression

H_2(ATSM), Ni^{II}(ATSM) and $CuCl_2$ were incorporated as controls for Cu^{II}(ATSM) to assess whether the ATSM backbone or Cu induced the observed up-regulation of P-gp. hCMEC/D3 cells were treated with vehicle (0.1% *(v/v)* DMSO) or 100 nM of Cu^{II}(ATSM), H_2(ATSM), Ni^{II}(ATSM) or 100 nM $CuCl_2$ for 24 h. Following treatment, cells were assessed for intracellular Cu levels by ICP-MS as well as P-gp protein and mRNA expression by Western blot and RT-qPCR, respectively, as described previously.

2.2.9 | Statistical analysis

All graphs and data were analysed using GraphPad Prism® software version 8.1.1 (GraphPad Software Incorporated). All comparisons between control and treatment groups were assessed by one-way analysis of variance (ANOVA) followed by a post hoc Dunnett's test that compared the mean of each treatment group to the mean of vehicle (0.1% *(v/v)* DMSO) treated groups or a

Tukey's test to compare the mean of each group to all other groups to correct for multiple comparisons. Levels of significance are indicated for individual experiments, with differences considered to be statistically significant when the *p value* was less than 0.05 ($p < 0.05$). n represents the number of biological replicates in the in vitro studies for independent cell culture preparations. Data were assessed for normality using the Sharpiro–Wilk test and all data points were used for statistical analysis and no sample size calculation was performed. These studies did not require institutional ethical approval and no blinding or randomisation was performed to allocate groups in the study. The outcomes of this study were exploratory and did not have any inclusion or exclusion criteria pre-determined.

3 | RESULTS

3.1 | hCMEC/D3 cells tolerate higher concentrations of Cu^{II}(ATSM) relative to Cu^{II}(GTSM)

As the impact of Cu^{II}(BTSC) compounds on hCMEC/D3 cell function had not been reported, it was essential to establish appropriate concentrations for treatments that did not negatively affect cell viability or morphology. Morphological assessment and MTT assays were used to assess cellular viability, whereas extracellular LDH activity was assessed to measure cytotoxicity and ensure detached cells were indeed undergoing cellular damage. Concentrations of up to 250 nM of each compound did not elicit toxicity up to 48 h (Figure 1e, f), after which, toxicity was observed with both MTT and LDH assays, outcomes confirmed by morphological assessment (Figure 1). However, even at 72 h, Cu^{II}(ATSM) did not generate cell toxicity until 500 nM for both MTT and LDH assays (Figure 1d, f). For Cu^{II}(ATSM), the MTT assay results were concordant with those obtained by the LDH assay. Cu^{II}(GTSM) induced toxicity at 72 h at all concentrations, as assessed by the MTT assay and concentrations above 250 nM led to a significant increase in extracellular LDH activity indicating damage to the membrane of cells (Figure 1c, e). hCMEC/D3 cells that were treated with 250 nM of Cu^{II}(ATSM) for 72 h appeared morphologically similar to vehicle-treated hCMEC/D3 cells (Figure 1g, h), whereas 250 nM of Cu^{II}(GTSM) caused a significant decrease in viable cells as observed by the presence of detached cell debris (Figure 1i). All concentrations of Cu^{II}(ATSM) and Cu^{II}(GTSM) were not toxic at 8, 24 and 48 h, except for 500 nM Cu^{II}(GTSM) at 24 and 48 h. Based on these results, subsequent studies only assessed the impact of Cu^{II}(ATSM) and Cu^{II}(GTSM) at concentrations of 25–250 nM over 8–48 h.

3.2 | Cu^{II}(ATSM) enhances P-gp expression while Cu^{II}(GTSM) decreases P-gp expression in hCMEC/D3 cells

Three different concentrations (25, 100 and 250 nM) of both Cu^{II}(ATSM) and Cu^{II}(GTSM) were used to assess whether these compounds modulate P-gp expression in hCMEC/D3 cells in a concentration-dependent manner over 8–48 h. Cu^{II}(ATSM) was initially used as a negative control given that this complex does not readily release bioavailable Cu under normoxic conditions. There were no significant changes in hCMEC/D3 expression of P-gp following 8 h treatments with either of the two compounds (Figure 2a). However, following 24 and 48 h treatments, the expression of P-gp in hCMEC/D3 cells treated with Cu^{II}(ATSM) at 25, 100 and 250 nM was significantly increased, with densitometric analysis demonstrating a 1.5–2.0 fold increase relative to vehicle-treated hCMEC/D3 cells (Figure 2b and c). In comparison, all concentrations of Cu^{II}(GTSM) did not significantly modulate P-gp expression following a 24 h treatment, and in fact, at 48 h it was shown that Cu^{II}(GTSM) treatment significantly reduced the abundance of P-gp protein in hCMEC/D3 cells (Figure 2c).

3.3 | Cu^{II}(BTSC)-mediated alterations to P-gp protein expression correlated with modified efflux capacity in hCMEC/D3 cells

The efflux function of P-gp was assessed using an assay employing a known fluorescent P-gp substrate R123, to determine if the observed increase or decrease in P-gp expression resulted in enhanced or reduced efflux capacity, respectively. PSC833, an inhibitor of P-gp (5 μM), was used to ensure that efflux of R123 could be blocked, which was indeed observed in all functional studies (Figure 3). A 24 h treatment with Cu^{II}(ATSM) at 25, 100 and 250 nM concentrations led to reduced accumulation of R123 by approximately 23–31% when compared with vehicle-treated cells (Figure 3a), consistent with the observed up-regulation of P-gp with this compound. This reduction was also observed after 48 h treatments with Cu^{II}(ATSM) (25–250 nM) albeit to a lesser extent (approximately 15–21% reduction when compared with controls) (Figure 3c). The reduced accumulation of R123 in response to Cu^{II}(ATSM) was able to be inhibited with the presence of PSC833 inhibitor similar to that of PSC833 alone suggesting that enhanced efflux mediated by Cu^{II}(ATSM) is likely through P-gp and not via the functional modification of other efflux transporters (Figure 3a). In contrast to that observed with Cu^{II}(ATSM), and in line with the reduction in P-gp expression, Cu^{II}(GTSM) increased R123 accumulation. Following 24 h treatment with 100 nM and 250 nM Cu^{II}(GTSM), a 26–36% increase in accumulation was observed (Figure 3b) and this effect was more pronounced with 48 h treatments to an extent that appeared more substantial than the effect of PSC833 (Figure 3d). As it could be argued that the effect of Cu^{II}(GTSM) could be a result of direct inhibition of P-gp, R123 uptake was measured in the presence and absence of Cu^{II}(GTSM) without a 24 or 48 h pre-treatment. While PSC833 increased hCMEC/D3 cellular accumulation of R123, co-incubation of Cu^{II}(GTSM) and R123 did not significantly alter R123 accumulation, indicating no competitive inhibition of P-gp-mediated efflux by Cu^{II}(GTSM) (Figure 3e).

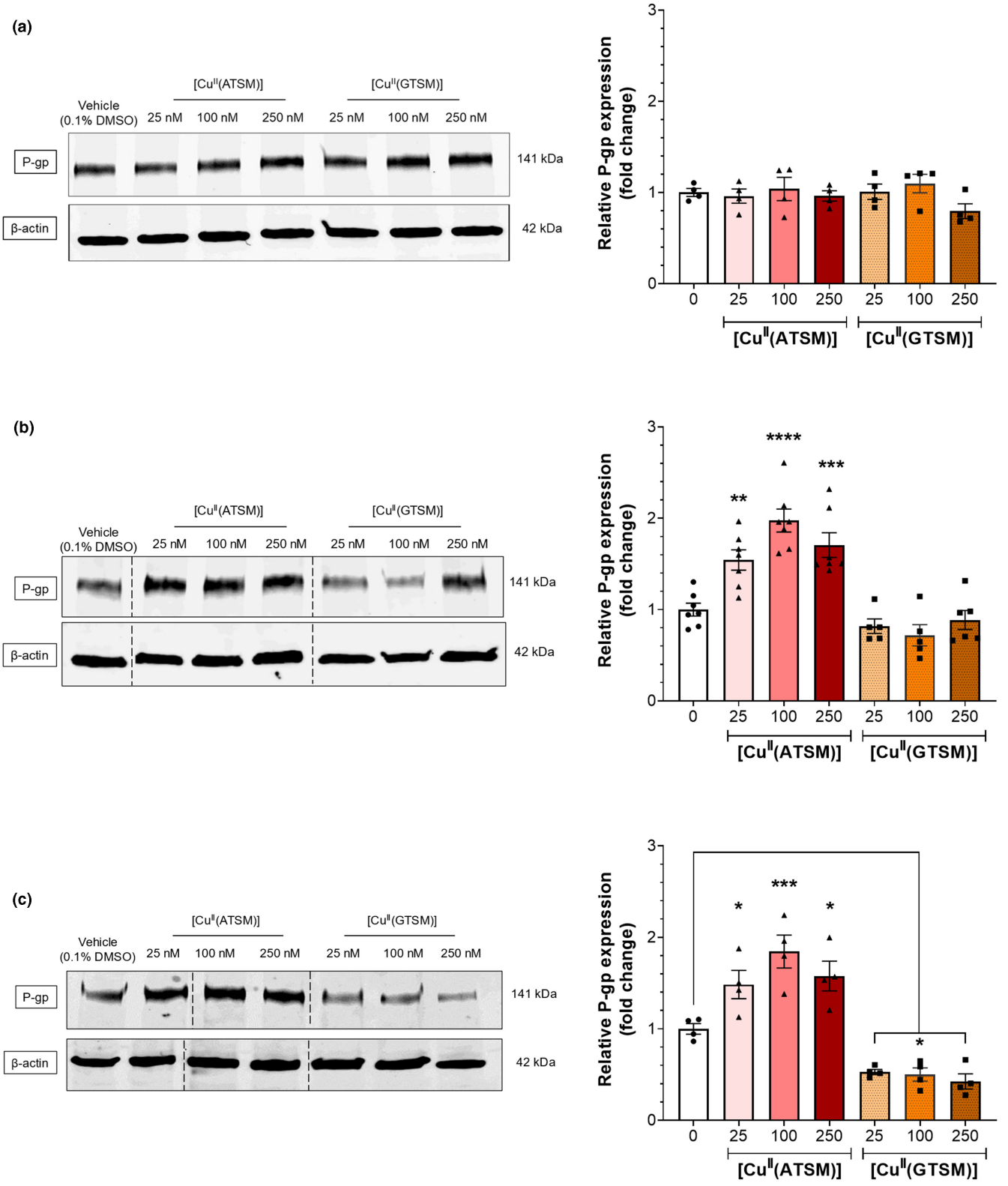

FIGURE 2 Cu^{II}(ATSM) up-regulates P-gp expression, while Cu^{II}(GTSM) attenuates P-gp expression, in hCMEC/D3 cells. Representative Western blots of expression levels of P-gp and β-actin in hCMEC/D3 cells grouped from single gel (--- dividing lines indicate reordered treatment lanes for presentation purposes) (left) and graphical representation of P-gp expression as assessed by densitometry (right) for (a) 8 h, (b) 24 h and (c) 48 h treatment with Cu^{II}(ATSM) or Cu^{II}(GTSM). Data are presented as mean ± SEM ($n = 4–7$, for independent cell culture preparations) expressed as fold change of vehicle (0.1% *(v/v)* DMSO), $^{*}p < 0.05$, $^{**}p < 0.01$, $^{***}p < 0.001$, $^{****}p < 0.0001$ when compared with vehicle-treated hCMEC/D3 cells, assessed by a one-way ANOVA followed by a post hoc Dunnett's test

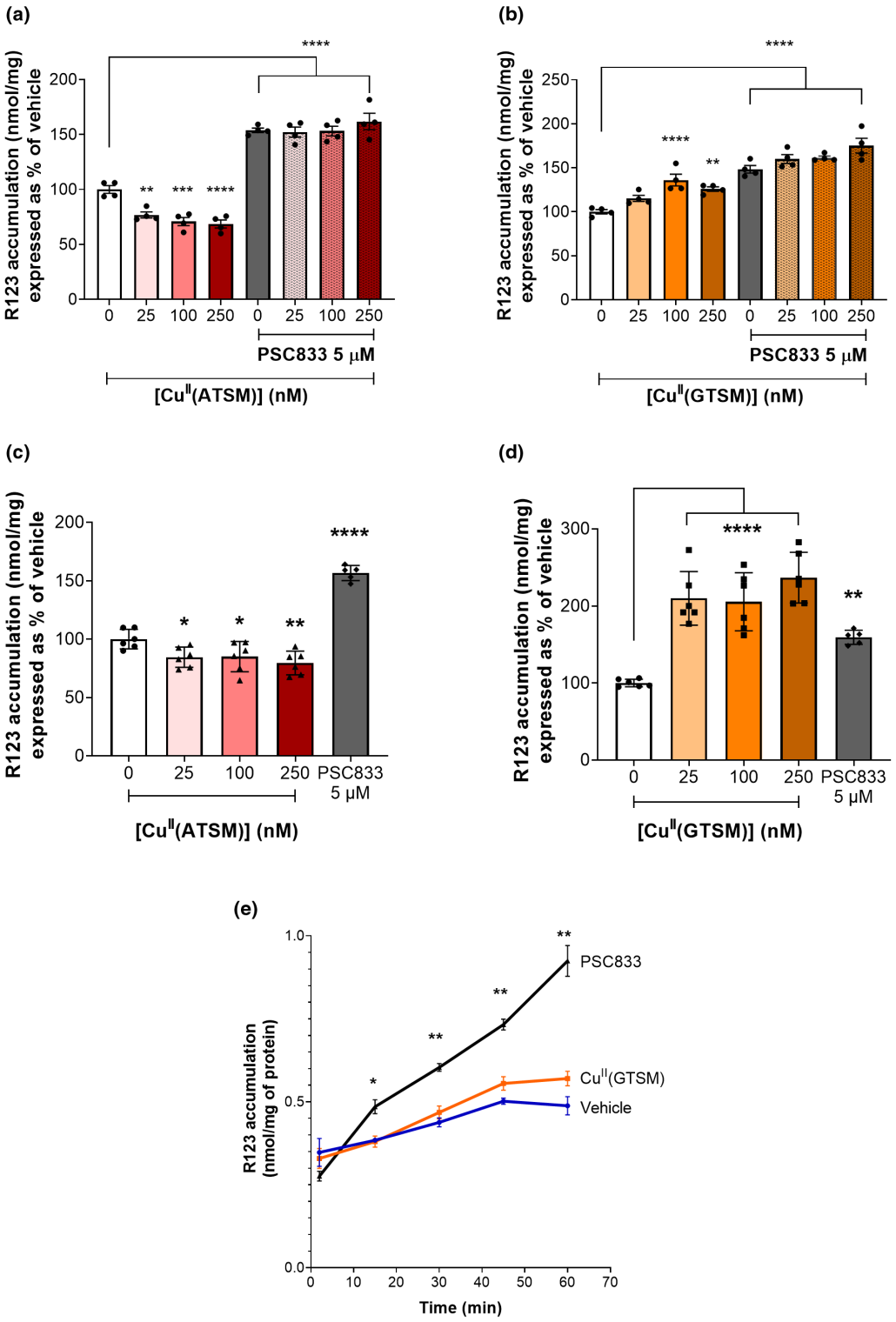

FIGURE 3 Cu^{II}(ATSM) reduces accumulation of R123 in hCMEC/D3 cells at 24 h (a) and 48 h (c), whereas Cu^{II}(GTSM) increases accumulation of R123 after (b) 24 h and (d) 48 h exposure. P-gp function was assessed by measuring the cellular accumulation of a fluorescent substrate, R123 (nmol), normalised to well protein (mg). The P-gp inhibitor PSC833 (5 μM) inhibited the Cu^{II}(ATSM)-mediated reduction in R123 accumulation (a and b). Cu^{II}(GTSM) increases R123 accumulation and this is to an extent greater than the P-gp inhibitor PSC833 (5 μM) after a 48 h treatment (c and d). P-gp-mediated accumulation of R123 was not affected by co-exposure with Cu^{II}(GTSM) (100 nM) over a 60 min incubation (e). Data are presented as mean ± SEM ($n = 4–6$, independent cell culture preparations) for accumulation of R123 expressed as % of vehicle (0.1% *(v/v)* DMSO) (a–d) or nmol/mg of R123/protein (e). $^{*}p < 0.05$, $^{**}p < 0.01$, $^{***}p < 0.001$, $^{****}p < 0.0001$ when compared with vehicle assessed by a one-way ANOVA, followed by a post hoc Dunnett's test (for each time point for (c))

3.4 | Modulation of P-gp protein by Cu^{II}(BTSC) occurs via a transcriptional mechanism

To assess whether the observed changes to P-gp protein and function mediated by Cu^{II}(BTSC) complexes were due to modulation of MDR1 transcriptional mechanisms and not via potential protein degradation pathways, MDR1 mRNA was quantified by RT-qPCR following each treatment. These studies were conducted with 100 nM of Cu^{II}(ATSM) or Cu^{II}(GTSM) as a representative concentration for those used to demonstrate an increase in protein expression. Figure 4 represents pooled data from different treatment times each with their own Cu^{II}(ATSM) or Cu^{II}(GTSM) treatments as well as corresponding vehicle controls. At 8 h, there was no significant change to MDR1 mRNA following treatment with either Cu^{II}(ATSM) or Cu^{II}(GTSM). In line with increased protein abundance, Cu^{II}(ATSM) treatment for 16 and 24 h resulted in a significant increase in MDR1 mRNA, an effect not observed with Cu^{II}(GTSM). Interestingly, after a 48 h treatment with Cu^{II}(ATSM), the increase in MDR1 mRNA was no longer evident, however, at this time, the observed down-regulation in P-gp protein in response to Cu^{II}(GTSM) was associated with a down-regulation of MDR1 mRNA.

3.5 | Both Cu^{II}(ATSM) and Cu^{II}(GTSM) increase intracellular copper levels in hCMEC/D3 cells

Treatment with Cu^{II}(ATSM) was not predicted to lead to enhanced P-gp expression and function given that this compound has been reported to not readily release Cu under normoxic conditions. Furthermore, the compound previously reported to release Cu (i.e. Cu^{II}(GTSM)) either had no effect or reduced the expression and function of P-gp in hCMEC/D3 cells. To assess if the unexpected responses were associated with changes in intracellular levels of Cu, ICP-MS was employed. As expected, a 24 h treatment with 50 nM, 100 nM and 250 nM Cu^{II}(GTSM) significantly increased intracellular Cu levels by 5, 8, and 15-fold, respectively, compared to vehicle controls (Figure 5a). Unexpectedly, higher concentrations (i.e. 100 and 250 nM) of Cu^{II}(ATSM) also led to 6 and 10-fold increase in Cu, respectively (Figure 5a), suggesting that both compounds were able to deliver exogenous Cu into hCMEC/D3 cells. However, as the ICP-MS technique measures total Cu, whether the Cu was released as free bioavailable Cu or still bound to the backbone structure of the complexes remains to be identified.

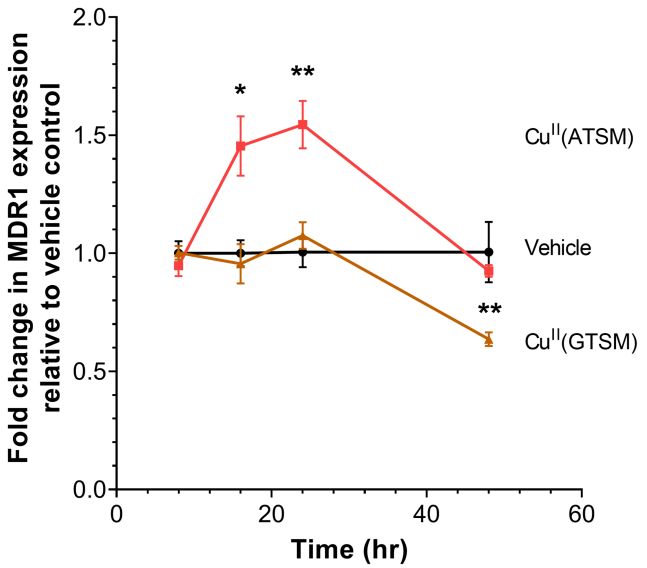

FIGURE 4 Time-dependent MDR1 mRNA expression in hCMEC/D3 cells following treatment with 100 nM Cu^{II}(ATSM) or Cu^{II}(GTSM). Data are presented as mean ± SEM ($n = 4$, independent cell culture preparations) expressed as fold-change relative to vehicle (0.1% *(v/v)* DMSO) for each timepoint. $^{*}p < 0.05$, $^{**}p < 0.01$ when compared with vehicle as assessed by a one-way ANOVA followed by a post hoc Dunnett's test for each timepoint

3.6 | Only Cu-ATSM and neither the ATSM backbone or Cu alone up-regulate P-gp expression

The ICP-MS data suggest that it is unlikely that exogenous Cu delivered from the Cu^{II}(ATSM) complex mediated the enhanced P-gp expression and function. To ascertain whether the observed P-gp effects may have been induced by the molecular ATSM backbone, independent of Cu, the effects of Ni^{II}(ATSM), H_2(ATSM) as well as $CuCl_2$ on P-gp expression were assessed. Following a 24 h treatment with each of the compounds, ICP-MS, Western blot and RT-qPCR were performed to quantify intracellular levels of Cu, P-gp protein expression and MDR1 mRNA expression, respectively. As expected, ICP-MS data showed increased intracellular Cu levels in hCMEC/D3 cells when treated with Cu^{II}(ATSM) or $CuCl_2$, while interestingly, Ni^{II}(ATSM) showed a reduction in Cu levels and H_2(ATSM) produced no significant changes in the levels of Cu (Figure 5b). If Cu was directly responsible for modulating P-gp expression, it would be predicted that $CuCl_2$ treatment would result in increased P-gp expression. Conversely, if the backbone structure of ATSM was responsible for the alterations in P-gp expression, then it would be expected that either the Ni^{II}(ATSM) or H_2(ATSM) would lead to changes in P-gp. However, Western blot and RT-qPCR data demonstrated that only Cu^{II}(ATSM) lead to an up-regulation of P-gp protein and mRNA (Figure 6), suggesting that the intact Cu and ATSM in the Cu^{II}(ATSM) complex elicits the observed responses and that independently they do not enhance P-gp expression.

3.7 | Cu^{II}(ATSM) induces phosphorylation of ERK1/2 leading to enhanced P-gp expression

Initially, it was thought that Cu would be responsible for increased P-gp expression, and that this may occur via activation of the Wnt/β-catenin and GSK3β pathway. As the results suggested that Cu was unlikely to be mediating the positive effects of Cu^{II}(ATSM),

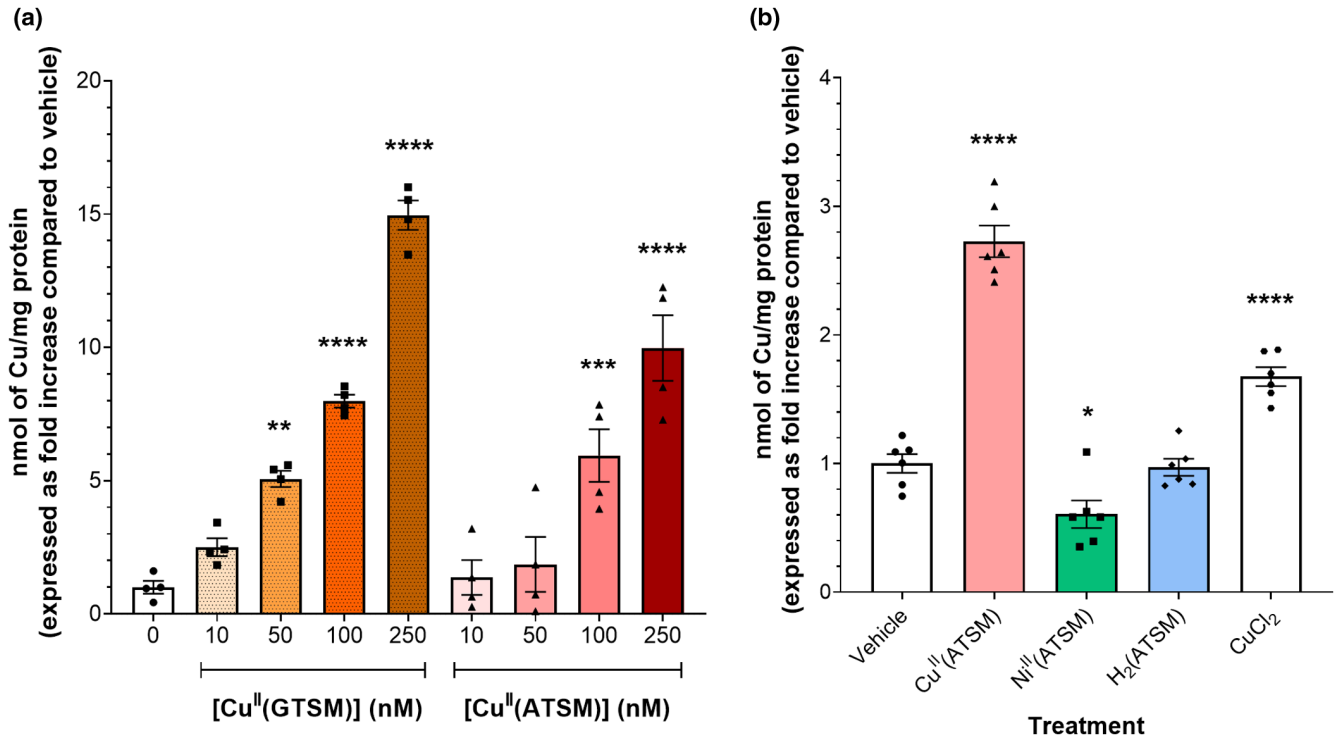

FIGURE 5 Intracellular Cu levels in hCMEC/D3 cells measured by ICP-MS following 24 h treatment with increasing concentrations of Cu^{II}(GTSM) or Cu^{II}(ATSM) (a) or with ATSM backbone derivatives and $CuCl_2$ (100 nM) (b). Data are presented as mean ± SEM ($n = 4–6$, independent cell culture preparations) as a fold change in Cu levels (normalised to protein) compared to vehicle (0.1% *(v/v)* DMSO). $^{*}p < 0.05$, $^{**}p < 0.01$, $^{***}p < 0.001$, $^{****}p < 0.0001$ when compared with vehicle-treated cells as assessed by a one-way ANOVA followed by a post hoc Dunnett's test

the role of ERK1/2 in mediating the effects of the BTSCs was explored. Interestingly both Cu^{II}(ATSM) and Cu^{II}(GTSM) induced phosphorylation of ERK1/2 in hCMEC/D3 cells 1.4 and 1.3 fold, respectively, when compared with vehicle (0.1% *(v/v)* DMSO) treated cells (Figure 7a, b). These effects were attenuated in the presence of a highly selective inhibitor of MEK1/2, an upstream kinase to ERK1/2 of the MAPK pathway (Figure 7). The presence of the MEK1/2 inhibitor U0126 significantly reduced MDR1 mRNA expression 0.3-fold compared to vehicle while the up-regulation observed with Cu^{II}(ATSM) was attenuated in the presence of this inhibitor to a similar (0.3 fold) extent (Figure 7c). This outcome builds confidence that ERK1/2 phosphorylation is involved in the Cu^{II}(ATSM)-mediated up-regulation of MDR1 mRNA given that inhibition of MEK1/2 and the subsequent inhibition of ERK1/2 phosphorylation partially attenuated the effect of Cu^{II}(ATSM) on MDR1 mRNA. It should be noted that the times chosen for assessing ERK1/2 phosphorylation differed between Cu^{II}(ATSM) and Cu^{II}(GTSM) (i.e. 24 and 48 h respectively) to ensure that any association between ERK phosphorylation and the compound of interest occurred when the compound exhibited effects on both mRNA and protein expression of P-gp.

The enhanced phosphorylation of ERK1/2 observed with Cu^{II}(GTSM) treatment did not accompany any changes in MDR1 mRNA expression (Figure 7d). Similarly, the presence of U0126 did not alter the previously observed down-regulation of MDR1 induced by a 48 h treatment with Cu^{II}(GTSM), suggesting that the effects of Cu^{II}(GTSM) on MDR1 down-regulation is unrelated to its effects on ERK1/2 phosphorylation.

4 | DISCUSSION

P-gp plays an imperative role in protecting the brain from a broad range of substrates, and while this poses a hindrance in delivering drugs across the BBB, P-gp is also implicated in AD as it has a key role in the clearance of the neurotoxic Aβ peptide from the brain (Cirrito et al., 2005; Deo et al., 2014; Hartz et al., 2010). Discovering potential modulators of P-gp expression and function and understanding the regulatory mechanisms involved in maintaining the function of this 'gatekeeper' has many potential applications to the development of neurotherapeutics. Cu has been demonstrated as essential for brain health as it influences multiple regulatory pathways within the CNS (Ayton et al., 2013; Lutsenko et al., 2010). Additionally, the biodistribution of Cu has been shown to be disrupted in AD (Ayton et al., 2013; Barnham & Bush, 2008; Barnham & Bush, 2014) but surprisingly little is known about the effects of Cu on brain endothelial cells despite this biometal requiring transport across the BBB to reach cells within the CNS. Given that Cu acts on pathways shown to be involved in P-gp regulation, this study was designed to identify whether enhancing the bioavailability of Cu chaperoned

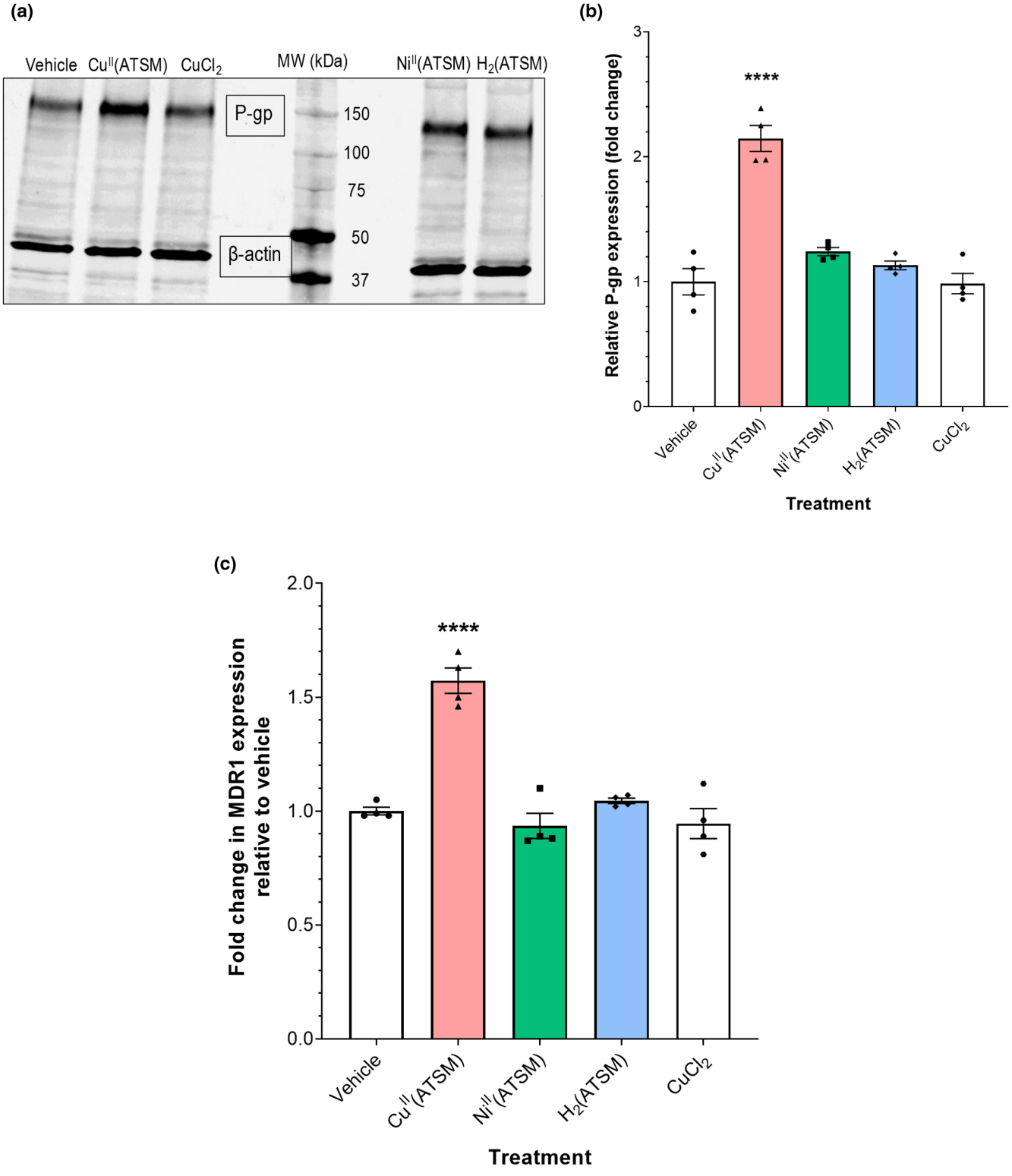

FIGURE 6 P-gp protein expression in hCMEC/D3 cells following a 24 h treatment with ATSM backbone derivatives or $CuCl_2$ (100 nM). Representative Western blot of expression levels of P-gp and β-actin in hCMEC/D3 cells with a molecular weight (MW) ladder as a reference for band weight from single gel (a) and graphical representation of P-gp expression as assessed by densitometry (b). MDR1 mRNA expression in hCMEC/D3 cells following a 24 h treatment (c). Data are presented as mean ± SEM ($n = 4$, independent cell culture preparations) expressed as a fold change to vehicle (0.1% *(v/v)* DMSO). ****$p < 0.0001$ when compared with the mean of all treatment groups as assessed by a one-way ANOVA followed by a post hoc Tukey's test

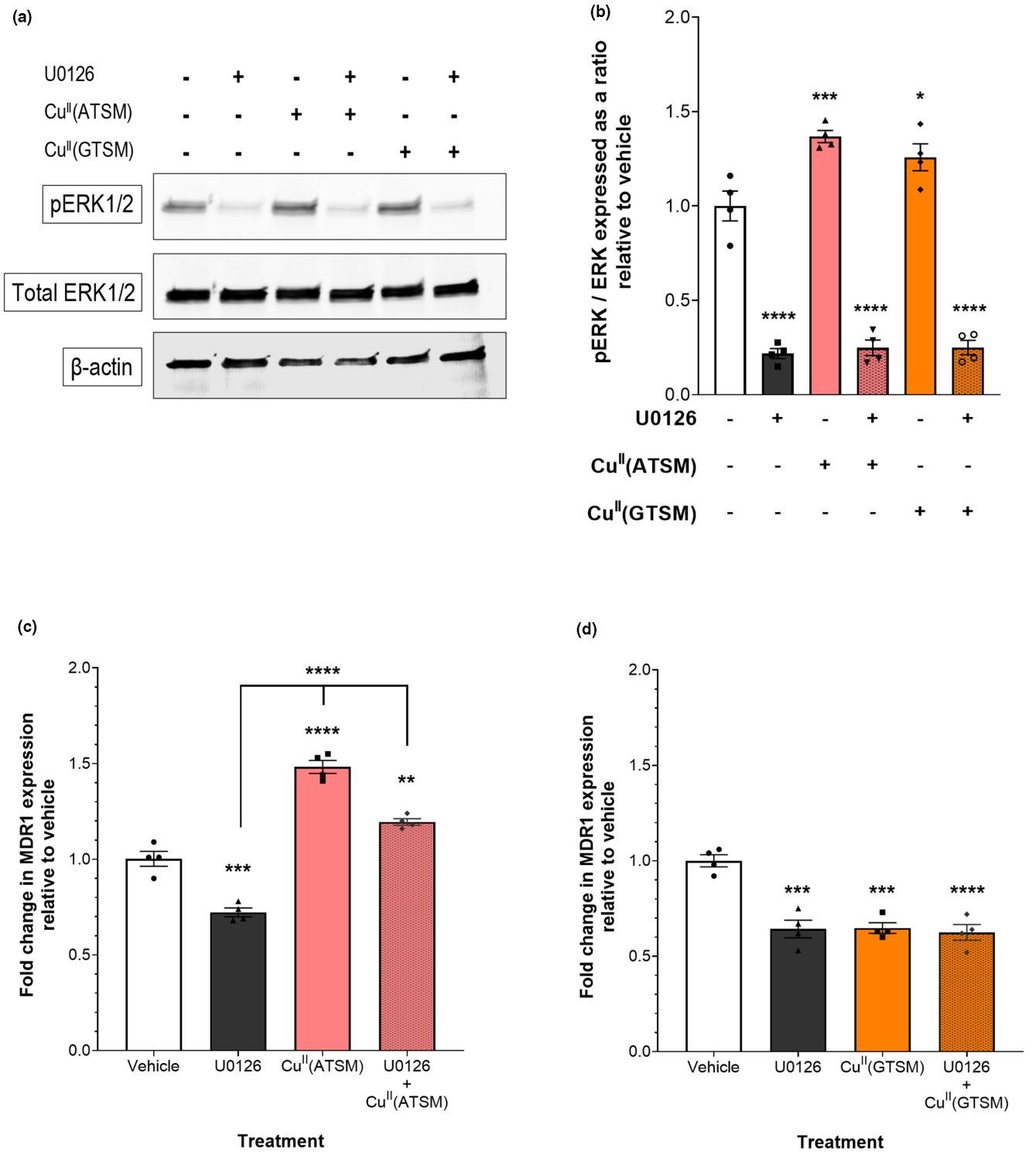

FIGURE 7 Both Cu^{II}(ATSM) and Cu^{II}(GTSM) mediated activation of ERK1/2 is attenuated by U0126, an inhibitor of MEK1/2. Representative Western blot of pERK1/2, ERK1/2 and β-actin in hCMEC/D3 cells from single gel (a) and graphical representation of pERK/ERK expression as assessed by densitometry (b) following treatment with combinations of Cu^{II}(ATSM) (100 nM) or Cu^{II}(GTSM) (100 nM) with or without U0126 (10 μM). MDR1 mRNA expression in hCMEC/D3 cells following a 24 h treatment with 100 nM of Cu^{II}(ATSM) with or without 10 μM of U0126 (c) and 48 h treatment with 100 nM of Cu^{II}(GTSM) with or without 10 μM of U0126 (d). Data are presented as mean ± SEM ($n = 4$, independent cell culture preparations) of pERK/ERK ratios as a fold change to vehicle (0.1% *(v/v)* DMSO) treatment (b) or fold change in MDR1 expression relative to vehicle (0.1% *(v/v)* DMSO) (c, d). *$p < 0.05$, **$p < 0.01$, ***$p < 0.001$, ****$p < 0.0001$ when compared with vehicle, as assessed by a one-way ANOVA followed by a post hoc Dunnett's test and panel compared to the mean of all other treatment groups as assessed by a one-way ANOVA followed by a post hoc Tukey's test

by Cu^{II}(BTSC) complexes could modulate the properties of P-gp in human brain endothelial cells.

The Cu^{II}(GTSM) complex was employed to enhance the delivery of Cu into hCMEC/D3 cells, while Cu^{II}(ATSM) was initially intended as a negative control as it has been previously shown to not readily release Cu under normal physiological conditions (Dearling et al., 2002; Xiao et al., 2008). These two compounds only differ in that Cu^{II}(ATSM) has two additional methyl groups (Figure 1b). Under normoxic conditions, Cu^{II}(GTSM) has a Cu^{2+}/Cu^{+} reduction potential of −0.44 V compared to Ag/AgCl, and the comparatively low reduction potential, relative to Cu^{II}(ATSM), allows intracellular reductants such as ascorbate and glutathione to reduce the Cu bound to Cu^{II}(GTSM) and hence release bioavailable Cu within cells (Xiao et al., 2008). The presence of the two methyl groups on Cu^{II}(ATSM) increases the reduction potential to −0.60 V and thus Cu^{II}(ATSM) has a more stable structure that does not readily release Cu (Xiao et al., 2008). However, under hypoxic conditions such as those in disease states where the intracellular environment has an increased reducing capacity, Cu^{II}(ATSM) is reduced and thus increases bioavailable Cu, making it a more selective compound for cells under oxygen-deprived stress (Dearling et al., 2002). The mechanism by which these compounds cross cell membranes, their subcellular trafficking, and how they regulate cellular responses is yet unknown. However, these BTSC compounds have immense potential as neurodegenerative therapeutics, and as diagnostic and imaging agents, with early clinical trials demonstrating promising outcomes in neurodegenerative diseases (Hilton et al., 2017; Hilton et al., 2020; Hung et al., 2012; Price et al., 2011; Southon et al., 2020; Williams et al., 2016). Therefore, while the BTSCs were used as model compounds to address the central question around whether Cu is involved in the regulation of P-gp at the BBB, they also have clinical potential and the findings from this study could provide additional insight into mechanisms associated with their benefits observed in disease models.

Our studies are the first to assess the impact of these compounds on hCMEC/D3 cells, a model of the BBB. It was shown that cell viability was compromised only at the highest concentration and longer treatment time for Cu^{II}(ATSM) and Cu^{II}(GTSM) suggesting metal-induced toxicity. The different responses in cell viability between Cu^{II}(ATSM) and Cu^{II}(GTSM) at the 72 h treatment times are likely associated with the differences in the release of bioavailable Cu in hCMEC/D3 cells as mentioned above, however, all subsequent experiments were performed at concentrations and treatment times that did not affect cellular viability and thus it is unlikely that the differences observed on expression and function on P-gp are attributed to differences observed on cellular viability in response to Cu^{II}(ATSM) or Cu^{II}(GTSM).

Any excess release of intracellular Cu by Cu^{II}(GTSM) that increases cytotoxicity is likely because of the formation of toxic free radicals caused by reactive oxygen species (ROS) as a result of the overloading Cu ions (Tabner et al., 2002). While our subsequent ICP-MS data suggest that both Cu^{II}(ATSM) and Cu^{II}(GTSM) increase cytosolic Cu in a concentration-dependent manner, it is difficult to ascertain whether these Cu measurements reflect free Cu or Cu still bound to the backbone structure of the BTSC complexes within cells. It has previously been demonstrated that APP-CHO cells treated with 25 μM Cu^{II}(ATSM) and Cu^{II}(GTSM) exhibited increased cellular Cu levels, that were 177-fold and 216-fold higher, respectively, when compared with vehicle controls (Donnelly et al., 2008). In line with our findings, another study has also shown decreased MTT reduction in pheochromocytoma cells 12 (PC12 cells) treated with 50 nM Cu^{II}(GTSM) for 18 h and this was not the case for Cu^{II}(ATSM), and they also observed a 3.1-fold increase in intracellular Cu (Bica et al., 2014), which is consistent with our ICP-MS data showing a 5-fold increase in intracellular Cu following Cu^{II}(GTSM) treatment. Therefore, the greater toxicity induced by Cu^{II}(GTSM) in hCMEC/D3 cells relative to Cu^{II}(ATSM) is in line with that reported for other cell types. When compared with other Cu^{II}(BTSC) complexes, Acevedo et al., demonstrated that Cu^{II}(GTSM) was the most efficient complex to increase intracellular Cu (Acevedo et al., 2018). Whether the dose-dependent increase in Cu is the bioavailable released form or complexed to the BTSC is yet to be determined, but it is hypothesised based on previous studies that the increase in Cu associated with Cu^{II}(ATSM) is complex-bound under normal physiological conditions, whereas the Cu associated with Cu^{II}(GTSM) is likely to be biologically active released Cu.

Based on previous data from our laboratory, elevated hCMEC/D3 Cu levels were associated with an increase in P-gp abundance (McInerney et al., 2018), and for this reason, it was hypothesised that Cu^{II}(GTSM) would enhance P-gp expression given the reported Cu-releasing properties of Cu^{II}(GTSM) relative to Cu^{II}(ATSM). However, Western blot analysis showed that treatment with Cu^{II}(ATSM) significantly increased P-gp protein abundance, whereas treatment with Cu^{II}(GTSM) diminished P-gp expression when cells were treated for longer periods. Functional studies confirmed that the observed up-regulation in P-gp expression in response to Cu^{II}(ATSM) was associated with enhanced efflux potential of this protein and Cu^{II}(GTSM) reduced P-gp-mediated efflux, in alignment with the P-gp down-regulating effect of this BTSC. The reduced accumulation of R123 in Cu^{II}(GTSM)-treated cells could have conceivably been a direct inhibitory effect of this compound on P-gp function and independent of changes to P-gp expression, given that Acevedo et al. (2018) suggested that Cu^{II}(GTSM) may be a P-gp substrate in HEK293 cell lines, and therefore could prevent P-gp-mediated efflux of R123. However, we confirmed that this was not the case as we performed R123 accumulation studies in the presence and absence of Cu^{II}(GTSM) (without the pre-incubation of Cu^{II}(GTSM) which reduces P-gp expression), and we demonstrated that R123 accumulation was not impacted by co-administration of Cu^{II}(GTSM). These data imply that the down-regulation in P-gp induced by Cu^{II}(GTSM) was more likely responsible for the increased accumulation of R123, rather than a direct inhibitory effect of Cu^{II}(GTSM) on P-gp activity. Overall, the findings from this study directly contradicted our initial hypothesis in that the Cu^{II}(GTSM) thought to enhance intracellular Cu reduced P-gp expression and function, whereas, the Cu^{II}(ATSM) reported to not release Cu actually enhanced P-gp expression and function.

To ascertain whether these unexpected results on P-gp protein were associated with transcriptional changes, MDR1 mRNA

expression was assessed. In line with the increase in P-gp protein levels, Cu^{II}(ATSM) increased MDR1 mRNA at 16 and 24 h, however, at the 48 h timepoint, the MDR1 promoter was no longer up-regulated which may indicate a depletion of the Cu^{II}(ATSM) mediated response or a recovery of the mRNA to an untreated state. Also in line with reducing P-gp protein levels, Cu^{II}(GTSM) reduced MDR1 mRNA at later time points, suggesting that the effect of Cu^{II}(GTSM) on P-gp protein occurred via a transcriptional mechanism. The central role of P-gp as the gatekeeper to the brain warrants having multiple pathways to regulate this important efflux transporter. Although extensive research has demonstrated the potential of biochemical substrates for P-gp, only a few key regulatory pathways have been characterised that include the pregnane X receptor (PXR), peroxisome proliferator-activated receptor (PPAR) and the canonical Wnt/β-catenin signalling pathways (Chan et al., 2011; Park et al., 2014; Zastre et al., 2009). The up-regulation of P-gp across these various signalling pathways share the common mechanism in that the activation of these pathways induces binding to DNA promoter regions for MDR1 and increases transcription of the MDR1 gene, coding for P-gp (Chan et al., 2011; Park et al., 2014; Zastre et al., 2009). One group treated hCMEC/D3 cells with an inhibitor of GSK-3β, 6-bromoindirubin-3′-oximine, for 16 h and this lead to an up-regulation of P-gp protein as well as activating the MDR1 promoter (Lim et al., 2008). Furthermore, another study showed that Cu^{II}(GTSM) inhibited GSK-3β leading to the activation of Wnt/β-catenin signalling, whereas Cu^{II}(ATSM) did not and this was attributed to the releasability of Cu (Crouch et al., 2009). However, since both Cu^{II}(ATSM) and Cu^{II}(GTSM) both increased Cu in hCMEC/D3 cells (with Cu^{II}(GTSM) releasing more Cu), it was likely that this pathway was not involved in the Cu^{II}(BTSC) effects on P-gp (Crouch et al., 2009). As the results suggested Cu was unlikely to be mediating the positive effects of Cu^{II}(ATSM), an alternative candidate pathway associated with the regulation of P-gp expression was explored. The MAPK pathway and the downstream activation of ERK1/2 has been positively correlated with the regulation of MDR1 transcription and subsequent P-gp expression (Nwaozuzu et al., 2003;Shao et al., 2016; Zhou et al., 2019), and this pathway has been shown to be activated by Cu^{II}(ATSM) and Cu^{II}(GTSM) (Acevedo et al., 2018; Crouch et al., 2009; Srivastava et al., 2016). Cu^{II}(ATSM) has been shown to phosphorylate ERK1/2 in human coronary artery smooth muscle cells (Srivastava et al., 2016) and by inhibiting this pathway, studies have shown reduced expression of P-gp (Shao et al., 2016; Zhou et al., 2019). Our studies demonstrated that Cu^{II}(ATSM) also induces phosphorylation of ERK1/2 in hCMEC/D3 cells and blockade of this pathway attenuated the effects of Cu^{II}(ATSM) on MDR1 mRNA, confirming that the effects of Cu^{II}(ATSM) on P-gp expression were mediated in part by the activation of MAPK signalling. Interestingly, Cu^{II}(GTSM) also enhanced the phosphorylation of ERK1/2, however, this was not accompanied by any changes in MDR1 mRNA expression, and furthermore, the presence of an inhibitor did not alter this down-regulation of MDR1, suggesting that the phosphorylation of ERK1/2 in response to Cu^{II}(GTSM) is unrelated to its effects on MDR1 regulation, and that additional factors or alternative pathways are involved in the MDR1 mRNA down-regulating effects of Cu^{II}(GTSM). Despite Cu^{II}(ATSM) and Cu^{II}(GTSM) both activating ERK1/2, their opposite effects on P-gp expression may be attributed to an increase in ROS levels associated with the readily released Cu from the Cu^{II}(GTSM) complex. Studies on P-gp regulation in tumour cells have reported that elevated ROS leads to activation of ERK1/2 as well as other kinases that share the same MAPK cascade of activation such as c-Jun N-terminal kinase (JNK) or p38, that act as negative regulators of P-gp expression (Wartenberg et al., 2001). Furthermore, the activation of JNK has been associated with down-regulation of P-gp in cerebral blood vessels despite maintaining integrity of BBB-associated proteins such as glucose transporter 1, zonula occludens-1 and occludin (Choi et al., 2019).

The positive effects of Cu^{II}(ATSM) on P-gp expression and function were unexpected, and suggested that Cu itself is not responsible for these effects given that Cu^{II}(GTSM), which also releases Cu, did not have such positive effects. If the observed up-regulation of P-gp is copper-independent, then it might be expected that the ATSM backbone structure of the complex may be acting independently to the release of Cu to induce P-gp expression and function. In line with this, Cu^{II}(ATSM) has been suggested to inhibit ferroptosis via a Cu-independent mechanism and the effects on ferroptosis were suggested to be driven by the ATSM backbone, given that Ni^{II}(ATSM) which has the same backbone structure (and does not release Cu) was shown to have a similar activity to Cu^{II}(ATSM) in preventing ferroptosis (Southon et al., 2020). For this reason, we assessed the impact of various backbone structures on MDR1 mRNA, using Ni^{II}(ATSM), H_2(ATSM) and $CuCl_2$. The Ni^{II}(ATSM) treatment served as a control for the compound with a non-biologically active divalent metal bound to the ATSM structure, while the H_2(ATSM) served as a pure ATSM structural control that has no biometal attached. $CuCl_2$ was included to confirm that Cu alone did not elicit changes to P-gp. These studies demonstrated that it was neither the backbone of ATSM, nor Cu alone, that increases MDR1 mRNA and P-gp protein, but that the combination of the Cu attached to the ATSM complex is what modulates the expression of P-gp in human brain endothelial cells. Whilst unexpected, this is a significant finding given that emerging research has shown that Cu^{II}(ATSM) has a neuroprotective role (Kuo et al., 2019; Shi et al., 2021) for multiple neurodegenerative diseases. Cu^{II}(ATSM), which is currently in clinical trials, could modulate P-gp expression and function and thus be used as a therapeutic tool to enhance CNS delivery of drugs, restore P-gp in neurodegenerative disease, and potentially enhance the clearance of Aβ in AD.

5 | CONCLUSION

This study demonstrated that Cu^{II}(ATSM) significantly increased the expression and function of P-gp in hCMEC/D3 cells through a transcriptional mechanism. The findings suggest that a combination of the Cu and ATSM structure in Cu^{II}(ATSM) mediated the observed effects, opening up a novel field of research to ascertain the pharmacological effects of this compound at the BBB. Unravelling any

role of Cu^{II}(BTSC) complexes in regulating P-gp will no doubt provide novel insight into the key biological processes crucial for the maintenance of the most important biological barrier that ensures the brain remains a protected reserve. This area of research has the potential to lead to unexploited targets at the BBB which can be pharmacologically manipulated and applied to neurodegenerative diseases including, but not limited to, AD.

ACKNOWLEDGEMENTS

Jae Pyun was supported by the Australian Government Research Training Program Scholarship. This study was also supported in part by funding from the Australian Research Council and the National Health and Medical Research Council. We thank the Mass Spectrometry and Proteomics Facility at Bio21 Institute, University of Melbourne. Collaborative Medicinal Development LLC has licenced intellectual property related to this subject from The University of Melbourne, where Professor Paul S. Donnelly is listed as an inventor and has served as a consultant to Collaborative Medicinal Development LLC. Professor Ashley I. Bush is a shareholder in Alterity Ltd, Cogstate Ltd and Mesoblast Ltd. He is a paid consultant for, and has a profit share interest in, Collaborative Medicinal Development LLC. Open access publishing facilitated by Monash University, as part of the Wiley - Monash University agreement via the Council of Australian University Librarians.

Correction added on 11th May 2022, after first online publication: CAUL funding statement has been added.

AUTHOR CONTRIBUTION

Jae Pyun conceived, planned and carried out all experiments, analysed experimental data, designed the figures and drafted the manuscript. Lachlan E. McInnes synthesised and characterised the bis(thiosemicarbazone) complexes. Celeste Mawal performed and processed the ICP-MS data. Paul S. Donnelly and Ashley I. Bush consulted on the study design, aided in interpreting the results and provided supervision of work. Jennifer L. Short and Joseph A. Nicolazzo were involved in designing, planning and supervised all aspects of the work. All authors discussed the results and commented on the manuscript.

DATA AVAILABILITY STATEMENT

The data that support the findings of this study are available from the corresponding author upon reasonable request.

ORCID

Ashley I. Bush https://orcid.org/0000-0001-8259-9069
Joseph A. Nicolazzo https://orcid.org/0000-0002-0983-7152

REFERENCES

Abbott, N. J., Patabendige, A. A., Dolman, D. E., Yusof, S. R., & Begley, D. J. (2010). Structure and function of the blood–brain barrier. *Neurobiology of Disease*, 37, 13–25.

Acevedo, K. M., Hayne, D. J., McInnes, L. E., Noor, A., Duncan, C., Moujalled, D., Volitakis, I., Rigopoulos, A., Barnham, K. J., Villemagne, V. L., White, A. R., & Donnelly, P. S. (2018). Effect of structural modifications to glyoxal-bis (thiosemicarbazonato) copper (II) complexes on cellular copper uptake, copper-mediated ATP7A trafficking, and P-glycoprotein mediated efflux. *Journal of Medicinal Chemistry*, 61, 711–723.

Atadja, P., Watanabe, T., Xu, H., & Cohen, D. (1998). PSC-833, a frontier in modulation of P-glycoprotein mediated multidrug resistance. *Cancer and Metastasis Reviews*, 17, 163–168.

Ayton, S., Lei, P., & Bush, A. I. (2013). Metallostasis in Alzheimer's disease. *Free Radical Biology and Medicine*, 62, 76–89.

Barnham, K. J., & Bush, A. I. (2008). Metals in Alzheimer's and Parkinson's diseases. *Current Opinion in Chemical Biology*, 12, 222–228.

Barnham, K. J., & Bush, A. I. (2014). Biological metals and metal-targeting compounds in major neurodegenerative diseases. *Chemical Society Reviews*, 43, 6727–6749.

Beraldo, H., Boyd, L. P., & West, D. X. (1997). Copper (II) and nickel (II) complexes of glyoxaldehyde bis {N (3)-substituted thiosemicarbazones}. *Transition Metal Chemistry*, 23, 67–71.

Bica, L., Liddell, J. R., Donnelly, P. S., Duncan, C., Caragounis, A., Volitakis, I., Paterson, B. M., Cappai, R., Grubman, A., Camakaris, J., Crouch, P. J., & White, A. R. (2014). Neuroprotective copper bis (thiosemicarbazonato) complexes promote neurite elongation. *PLoS One*, 9, e90070.

Blower, P. J., Castle, T. C., Cowley, A. R., Dilworth, J. R., Donnelly, P. S., Labisbal, E., Sowrey, F. E., Teat, S. J., & Went, M. J. (2003). Structural trends in copper (II) bis (thiosemicarbazone) radiopharmaceuticals. *Dalton Transactions*, 23, 4416–4425.

Callaghan, R., Luk, F., & Bebawy, M. (2014). Inhibition of the multidrug resistance P-glycoprotein: Time for a change of strategy? *Drug Metabolism and Disposition*, 42, 623–631.

Chai, A. B., Hartz, A., Gao, X., Yang, A., Callaghan, R., & Gelissen, I. C. (2021). New evidence for P-gp-mediated export of amyloid-β peptides in molecular, blood-brain barrier and neuronal models. *International Journal of Molecular Sciences*, 22, 246.

Chan, G. N., Hoque, M. T., Cummins, C. L., & Bendayan, R. (2011). Regulation of P-glycoprotein by orphan nuclear receptors in human brain microvessel endothelial cells. *Journal of Neurochemistry*, 118, 163–175.

Cherny, R. A., Atwood, C. S., Xilinas, M. E., Gray, D. N., Jones, W. D., McLean, C. A., Barnham, K. J., Volitakis, I., Fraser, F. W., Kim, Y. S., Huang, X., Goldstein, L. E., Moir, R. D., Lim, J. T., Beyreuther, K., Zheng, H., Tanzi, R. E., Masters, C. L., & Bush, A. I. (2001). Treatment with a copper-zinc chelator markedly and rapidly inhibits β-amyloid accumulation in Alzheimer's disease transgenic mice. *Neuron*, 30, 665–676.

Chiu, C., Miller, M. C., Monahan, R., Osgood, D. P., Stopa, E. G., & Silverberg, G. D. (2015). P-glycoprotein expression and amyloid accumulation in human aging and Alzheimer's disease: Preliminary observations. *Neurobiology of Aging*, 36, 2475–2482.

Choi, H., Lee, E.-H., Han, M., An, S.-H., & Park, J. (2019). Diminished expression of P-glycoprotein using focused ultrasound is associated with JNK-dependent signaling pathway in cerebral blood vessels. *Frontiers in Neuroscience*, 13, 1350.

Cirrito, J. R., Deane, R., Fagan, A. M., Spinner, M. L., Parsadanian, M., Finn, M. B., Jiang, H., Prior, J. L., Sagare, A., Bales, K. R., Paul, S. M., Zlokovic, B. V., Piwnica-Worms, D., & Holtzman, D. M. (2005). P-glycoprotein deficiency at the blood-brain barrier increases amyloid-β deposition in an Alzheimer disease mouse model. *The Journal of Clinical Investigation*, 115, 3285–3290.

Crouch, P. J., Hung, L. W., Adlard, P. A., Cortes, M., Lal, V., Filiz, G., Perez, K. A., Nurjono, M., Caragounis, A., du, T., Laughton, K., Volitakis, I., Bush, A. I., Li, Q. X., Masters, C. L., Cappai, R., Cherny, R. A., Donnelly, P. S., White, A. R., & Barnham, K. J. (2009). Increasing cu bioavailability inhibits Aβ oligomers and tau phosphorylation. *Proceedings of the National Academy of Sciences*, 106, 381–386.

Crouch, P. J., Savva, M. S., Hung, L. W., Donnelly, P. S., Mot, A. I., Parker, S. J., Greenough, M. A., Volitakis, I., Adlard, P. A., Cherny, R. A., Masters, C. L., Bush, A. I., Barnham, K. J., & White, A. R. (2011).

The Alzheimer's therapeutic PBT2 promotes amyloid-β degradation and GSK3 phosphorylation via a metal chaperone activity. *Journal of Neurochemistry*, 119, 220–230.

Dearling, J. L., Lewis, J. S., Mullen, G. E., Welch, M. J., & Blower, P. J. (2002). Copper bis (thiosemicarbazone) complexes as hypoxia imaging agents: Structure-activity relationships. *Journal of Biological Inorganic Chemistry*, 7, 249–259.

Deo, A. K., Borson, S., Link, J. M., Domino, K., Eary, J. F., Ke, B., Richards, T. L., Mankoff, D. A., Minoshima, S., O'Sullivan, F., Eyal, S., Hsiao, P., Maravilla, K., & Unadkat, J. D. (2014). Activity of P-glycoprotein, a β-amyloid transporter at the blood–brain barrier, is compromised in patients with mild Alzheimer disease. *Journal of Nuclear Medicine*, 55, 1106–1111.

Donnelly, P. S., Caragounis, A., Du, T., Laughton, K. M., Volitakis, I., Cherny, R. A., Sharples, R. A., Hill, A. F., Li, Q. X., Masters, C. L., Barnham, K. J., & White, A. R. (2008). Selective intracellular release of copper and zinc ions from bis(thiosemicarbazonato) complexes reduces levels of Alzheimer disease amyloid-β peptide. *Journal of Biological Chemistry*, 283, 4568–4577.

Gingras, B., Suprunchuk, T., & Bayley, C. H. (1962). The preparation of some thiosemicarbazones and their copper complexes: Part III. *Canadian Journal of Chemistry*, 40, 1053–1059.

Harati, R., Benech, H., Villégier, A. S., & Mabondzo, A. (2012). P-glycoprotein, breast cancer resistance protein, organic anion transporter 3, and transporting peptide 1a4 during blood–brain barrier maturation: Involvement of Wnt/β-catenin and endothelin-1 signaling. *Molecular Pharmaceutics*, 10, 1566–1580.

Hartz, A. M., Miller, D. S., & Bauer, B. (2010). Restoring blood-brain barrier P-glycoprotein reduces brain amyloid-β in a mouse model of Alzheimer's disease. *Molecular Pharmacology*, 77, 715–723.

Hawkins, B. T., & Davis, T. P. (2005). The blood-brain barrier/neurovascular unit in health and disease. *Pharmacological Reviews*, 57, 173–185.

Hickey, J. L., Crouch, P. J., Mey, S., Caragounis, A., White, J. M., White, A. R., & Donnelly, P. S. (2011). Copper (II) complexes of hybrid hydroxyquinoline-thiosemicarbazone ligands: GSK3β inhibition due to intracellular delivery of copper. *Dalton Transactions*, 40, 1338–1347.

Hilton, J. B., Kysenius, K., Liddell, J. R., Rautengarten, C., Mercer, S. W., Mercer, P., Beckman, J. S., McLean, C. A., White, A. R., Bush, A. I., Hare, D. J., Roberts, B. R., & Crouch, P. J. (2020). Disrupted copper availability in sporadic ALS: Implications for CuII (atsm) as a treatment option. *BioRxiv* (pre-print).

Hilton, J. B., Mercer, S. W., Lim, N. K. H., Faux, N. G., Buncic, G., Beckman, J. S., Roberts, B. R., Donnelly, P. S., White, A. R., & Crouch, P. J. (2017). CuII(atsm) improves the neurological phenotype and survival of SOD1G93A mice and selectively increases enzymatically active SOD1 in the spinal cord. *Scientific Reports*, 7, 42292–42303.

Hung, L. W., Villemagne, V. L., Cheng, L., Sherratt, N. A., Ayton, S., White, A. R., Crouch, P. J., Lim, S. C., Leong, S. L., Wilkins, S., George, J., Roberts, B. R., Pham, C. L. L., Liu, X., Chiu, F. C. K., Shackleford, D. M., Powell, A. K., Masters, C. L., Bush, A. I., … Barnham, K. J. (2012). The hypoxia imaging agent CuII (atsm) is neuroprotective and improves motor and cognitive functions in multiple animal models of Parkinson's disease. *Journal of Experimental Medicine*, 209, 837–854.

Jeynes, B., & Provias, J. (2011). An investigation into the role of P-glycoprotein in Alzheimer's disease lesion pathogenesis. *Neuroscience Letters*, 487, 389–393.

Jones, C. J., & McCleverty, J. A. (1971). Complexes of transition metals with Schiff bases and the factors influencing their redox properties. Part II. Nickel and cobalt complexes of some terdentate chelating ligands containing the donor atom set N2S. *Journal of the Chemical Society A: Inorganic, Physical, Theoretical*, 0, 38–43.

Juliano, R. L., & Ling, V. (1976). A surface glycoprotein modulating drug permeability in Chinese hamster ovary cell mutants. *Biochimica et Biophysica Acta (BBA)-Biomembranes*, 455, 152–162.

Kannan, P., Brimacombe, K. R., Zoghbi, S. S., Liow, J. S., Morse, C., Taku, A. K., Pike, V. W., Halldin, C., Innis, R. B., Gottesman, M. M., & Hall, M. D. (2010). N-desmethyl-loperamide is selective for P-glycoprotein among three ATP-binding cassette transporters at the blood-brain barrier. *Drug Metabolism and Disposition*, 38, 917–922.

Karamanos, Y., Gosselet, F., Dehouck, M.-P., & Cecchelli, R. (2014). Blood–brain barrier proteomics: Towards the understanding of neurodegenerative diseases. *Archives of Medical Research*, 45, 730–737.

Kuhnke, D., Jedlitschky, G., Grube, M., Krohn, M., Jucker, M., Mosyagin, I., Cascorbi, I., Walker, L. C., Kroemer, H. K., Warzok, R. W., & Vogelgesang, S. (2007). MDR1-P-glycoprotein (ABCB1) mediates transport of Alzheimer's amyloid-β peptides—Implications for the mechanisms of Aβ clearance at the blood–brain barrier. *Brain Pathology*, 17, 347–353.

Kuo, M. T., Beckman, J. S., & Shaw, C. A. (2019). Neuroprotective effect of CuATSM on neurotoxin-induced motor neuron loss in an ALS mouse model. *Neurobiology of Disease*, 130, 104495.

Kusuhara, H., Suzuki, H., Terasaki, T., Kakee, A., Lemaire, M., & Sugiyama, Y. (1997). P-glycoprotein mediates the efflux of quinidine across the blood-brain barrier. *Journal of Pharmacology and Experimental Therapeutics*, 283, 574–580.

Lam, F. C., Liu, R., Lu, P., Shapiro, A. B., Renoir, J. M., Sharom, F. J., & Reiner, P. B. (2001). β-Amyloid efflux mediated by P-glycoprotein. *Journal of Neurochemistry*, 76, 1121–1128.

Lim, J. C., Kania, K. D., Wijesuriya, H., Chawla, S., Sethi, J. K., Pulaski, L., Romero, I. A., Couraud, P. O., Weksler, B. B., Hladky, S. B., & Barrand, M. A. (2008). Activation of β-catenin signalling by GSK-3 inhibition increases P-glycoprotein expression in brain endothelial cells. *Journal of Neurochemistry*, 106, 1855–1865.

Livak, K. J., & Schmittgen, T. D. (2001). Analysis of relative gene expression data using real-time quantitative PCR and the $2^{-\Delta\Delta CT}$ method. *Methods*, 25, 402–408.

Lutsenko, S., Bhattacharjee, A., & Hubbard, A. L. (2010). Copper handling machinery of the brain. *Metallomics*, 2, 596–608.

McInerney, M. P., Volitakis, I., Bush, A. I., Banks, W. A., Short, J. L., & Nicolazzo, J. A. (2018). Ionophore and biometal modulation of P-glycoprotein expression and function in human brain microvascular endothelial cells. *Pharmaceutical Research*, 35, 83.

Nicolazzo, J. A., Charman, S. A., & Charman, W. N. (2006). Methods to assess drug permeability across the blood-brain barrier. *Journal of Pharmacy and Pharmacology*, 58, 281–293.

Nwaozuzu, O. M., Sellers, L. A., & Barrand, M. A. (2003). Signalling pathways influencing basal and H_2O_2-induced P-glycoprotein expression in endothelial cells derived from the blood–brain barrier. *Journal of Neurochemistry*, 87, 1043–1051.

Palmeira, A., Sousa, E., Vasconcelos, M. H., & Pinto, M. M. (2012). Three decades of P-gp inhibitors: Skimming through several generations and scaffolds. *Current Medicinal Chemistry*, 19, 1946–2025.

Park, R., Kook, S., Park, J., & Mook-Jung, I. (2014). Aβ 1–42 reduces P-glycoprotein in the blood–brain barrier through RAGE–NF-κB signaling. *Cell Death & Disease*, 5, e1299.

Price, K. A., Crouch, P. J., Lim, S., Paterson, B. M., Liddell, J. R., Donnelly, P. S., & White, A. R. (2011). Subcellular localization of a fluorescent derivative of cu II (atsm) offers insight into the neuroprotective action of cu II (atsm). *Metallomics*, 3, 1280–1290.

Qosa, H., Lichter, J., Sarlo, M., Markandaiah, S. S., McAvoy, K., Richard, J. P., Jablonski, M. R., Maragakis, N. J., Pasinelli, P., & Trotti, D. (2016). Astrocytes drive upregulation of the multidrug resistance transporter ABCB1 (P-glycoprotein) in endothelial cells of the blood–brain barrier in mutant superoxide dismutase 1-linked amyotrophic lateral sclerosis. *Glia*, 64, 1298–1313.

Schinkel, A. H., Smit, J. J. M., van Tellingen, O., Beijnen, J. H., Wagenaar, E., van Deemter, L., Mol, C. A., van der Valk, M. A., Robanus-Maandag, E. C., te Riele, H. P., Berns, A. J. M., & Borst, P. (1994).

Disruption of the mouse mdr1a P-glycoprotein gene leads to a deficiency in the blood-brain barrier and to increased sensitivity to drugs. *Cell*, 77, 491–502.

Schinkel, A. H. (1999). P-glycoprotein, a gatekeeper in the blood–brain barrier. *Advanced Drug Delivery Reviews*, 36, 179–194.

Schinkel, A. H., Wagenaar, E., Mol, C. A., & van Deemter, L. (1996). P-glycoprotein in the blood-brain barrier of mice influences the brain penetration and pharmacological activity of many drugs. *The Journal of Clinical Investigation*, 97, 2517–2524.

Schinkel, A. H., Wagenaar, E., van Deemter, L., Mol, C., & Borst, P. (1995). Absence of the mdr1a P-glycoprotein in mice affects tissue distribution and pharmacokinetics of dexamethasone, digoxin, and cyclosporin a. *The Journal of Clinical Investigation*, 96, 1698–1705.

Shao, Y., Wang, C., Hong, Z., & Chen, Y. (2016). Inhibition of p38 mitogen-activated protein kinase signaling reduces multidrug transporter activity and anti-epileptic drug resistance in refractory epileptic rats. *Journal of Neurochemistry*, 136, 1096–1105.

Shen, D. Y., Zhang, W., Zeng, X., & Liu, C. Q. (2013). Inhibition of Wnt/β-catenin signaling downregulates P-glycoprotein and reverses multi-drug resistance of cholangiocarcinoma. *Cancer Science*, 104, 1303–1308.

Shi, X., Ohta, Y., Nakano, Y., Liu, X., Tadokoro, K., Feng, T., Nomura, E., Tsunoda, K., Sasaki, R., Matsumoto, N., Osakada, Y., Bian, Y., Bian, Z., Omote, Y., Takemoto, M., Hishikawa, N., Yamashita, T., & Abe, K. (2021). Neuroprotective effect of CuATSM in mice stroke model by ameliorating oxidative stress. *Neuroscience Research*, 166, 55–61.

Southon, A., Szostak, K., Acevedo, K. M., Dent, K. A., Volitakis, I., Belaidi, A. A., Barnham, K. J., Crouch, P. J., Ayton, S., Donnelly, P. S., & Bush, A. I. (2020). CuII (atsm) inhibits ferroptosis: Implications for treatment of neurodegenerative disease. *British Journal of Pharmacology*, 177, 656–667.

Srivastava, S., Blower, P. J., Aubdool, A. A., Hider, R. C., Mann, G. E., & Siow, R. C. (2016). Cardioprotective effects of cu (II) ATSM in human vascular smooth muscle cells and cardiomyocytes mediated by Nrf2 and DJ-1. *Scientific Reports*, 6, 1–13.

Tabner, B. J., Turnbull, S., El-Agnaf, O. M., & Allsop, D. (2002). Formation of hydrogen peroxide and hydroxyl radicals from Aβ and α-synuclein as a possible mechanism of cell death in Alzheimer's disease and Parkinson's disease. *Free Radical Biology and Medicine*, 32, 1076–1083.

Ueda, K., Clark, D., Chen, C., Roninson, I., Gottesman, M., & Pastan, I. (1987). The human multidrug resistance (mdr1) gene. cDNA cloning and transcription initiation. *Journal of Biological Chemistry*, 262, 505–508.

van Assema, D. M. E., Lubberink, M., Bauer, M., van der Flier, W. M., Schuit, R. C., Windhorst, A. D., Comans, E. F. I., Hoetjes, N. J., Tolboom, N., Langer, O., Müller, M., Scheltens, P., Lammertsma, A. A., & van Berckel, B. N. M. (2012). Blood–brain barrier P-glycoprotein function in Alzheimer's disease. *Brain*, 135, 181–189.

Vautier, S., & Fernandez, C. (2009). ABCB1: The role in Parkinson's disease and pharmacokinetics of antiparkinsonian drugs. *Expert Opinion on Drug Metabolism & Toxicology*, 5, 1349–1358.

Vogelgesang, S., Cascorbi, I., Schroeder, E., Pahnke, J., Kroemer, H. K., Siegmund, W., Kunert-Keil, C., Walker, L. C., & Warzok, R. W. (2002). Deposition of Alzheimer's β-amyloid is inversely correlated with P-glycoprotein expression in the brains of elderly non-demented humans. *Pharmacogenetics and Genomics*, 12, 535–541.

Wartenberg, M., Ling, F. C., Schallenberg, M., Bäumer, A. T., Petrat, K., Hescheler, J. R., & Sauer, H. (2001). Down-regulation of intrinsic P-glycoprotein expression in multicellular prostate tumor spheroids by reactive oxygen species. *Journal of Biological Chemistry*, 276, 17420–17428.

Weksler, B. B., Subileau, E. A., Perrière, N., Charneau, P., Holloway, K., Leveque, M., Tricoire-Leignel, H., Nicotra, A., Bourdoulous, S., Turowski, P., Male, D. K., Roux, F., Greenwood, J., Romero, I. A., & Couraud, P. O. (2005). Blood-brain barrier-specific properties of a human adult brain endothelial cell line. *The FASEB Journal*, 19, 1872–1874.

West, D. X., Ives, J. S., Bain, G. A., Liberta, A. E., Valdés-Martínez, J., Ebert, K. H., & Hernández-Ortega, S. (1997). Copper (II) and nickel (II) complexes of 2, 3-butanedione bis (N (3)-substituted thiosemicarbazones). *Polyhedron*, 16, 1895–1905.

Wijesuriya, H. C., Bullock, J. Y., Faull, R. L., Hladky, S. B., & Barrand, M. A. (2010). ABC efflux transporters in brain vasculature of Alzheimer's subjects. *Brain Research*, 1358, 228–238.

Williams, J. R., Trias, E., Beilby, P. R., Lopez, N. I., Labut, E. M., Bradford, C. S., Roberts, B. R., McAllum, E. J., Crouch, P. J., Rhoads, T. W., Pereira, C., Son, M., Elliott, J. L., Franco, M. C., Estévez, A. G., Barbeito, L., & Beckman, J. S. (2016). Copper delivery to the CNS by CuATSM effectively treats motor neuron disease in SODG93A mice co-expressing the copper-chaperone-for-SOD. *Neurobiology of Disease*, 89, 1–9.

Xiao, Z., Donnelly, P. S., Zimmermann, M., & Wedd, A. G. (2008). Transfer of copper between bis (thiosemicarbazone) ligands and intracellular copper-binding proteins. Insights into mechanisms of copper uptake and hypoxia selectivity. *Inorganic Chemistry*, 47, 4338–4347.

Zastre, J. A., Chan, G. N., Ronaldson, P. T., Ramaswamy, M., Couraud, P. O., Romero, I. A., Weksler, B., Bendayan, M., & Bendayan, R. (2009). Up-regulation of P-glycoprotein by HIV protease inhibitors in a human brain microvessel endothelial cell line. *Journal of Neuroscience Research*, 87, 1023–1036.

Zhou, Y., Zhou, J., Li, P., Xie, Q., Sun, B., Li, Y., Chen, Y., Zhao, K., Yang, T., Zhu, L., Xu, J., Liu, X., & Liu, L. (2019). Increase in P-glycoprotein levels in the blood-brain barrier of partial portal vein ligation/chronic hyperammonemia rats is medicated by ammonia/reactive oxygen species/ERK1/2 activation: In vitro and in vivo studies. *European Journal of Pharmacology*, 846, 119–127.

SUPPORTING INFORMATION

Additional supporting information may be found in the online version of the article at the publisher's website.

How to cite this article: Pyun, J., McInnes, L.E., Donnelly, P.S., Mawal, C., Bush, A.I., Short, J.L., & Nicolazzo, J. A. (2022). Copper bis(thiosemicarbazone) complexes modulate P-glycoprotein expression and function in human brain microvascular endothelial cells. *Journal of Neurochemistry*, 162, 226–244. https://doi.org/10.1111/jnc.15609